Three-dimensional ordering in bct antiferromagnets due to quantum disorder

T. Yildirim
University of Maryland, College Park, Maryland 20742;
National Institute of Standards and Technology, Gaithersburg, Maryland 20899;
and Department of Physics, University of Pennsylvania, Philadelphia, Pennsylvania 19104

A. B. Harris
Department of Physics, University of Pennsylvania, Philadelphia, Pennsylvania 19104;
Theoretical Physics, Oxford University, Oxford, OX2 3NP, United Kingdom;
and School of Physics and Astronomy, Raymond and Beverly Sackler Institute of Exact Sciences, Tel Aviv University, Tel Aviv 69978, Israel

E. F. Shender
Department of Physics, University of California, Berkeley, California 94720
and Institute of Nuclear Physics, St. Petersburg, Russia
(Received 11 August 1995)

Quantum effects on magnetic ordering in body-centered-tetragonal antiferromagnets with only nearest-neighbor interactions are studied in detail using interacting spin-wave theory. The model consists of M noninteracting (in a mean-field sense) antiferromagnetic planes which together form a body-centered-tetragonal structure. We obtain the leading quantum correction of order $1/S$ from the zero-point energy for a system of M planes whose staggered moments have arbitrary orientations. The infinite degeneracy of the ground-state manifold of this system is partially removed by collinear ordering in view of effects previously calculated by Shender at relative order $J_\perp^2/(J^2S)$, where J, the antiferromagnetic in-plane exchange interaction, is assumed to dominate $J_\perp$, the out-of-plane interaction which can be of either sign. We study the complete removal of the remaining degeneracy of the collinear spin structures by assigning an arbitrary sign σ_i $(i=1,2,\ldots M)$ to the staggered moment of the planes. Our result for the zero-point energy (for $M>2$) up to the sixth order in $j=J_\perp/J$ is

$$E(\{\sigma_i\})=E_1+CE_G(j^6/S)\left[-2\sigma_1\sigma_3-2\sigma_{M-2}\sigma_M+2\sum_{i=1}^{M-2}\sigma_i\sigma_{i+2}-3\sum_{i=1}^{M-3}\sigma_i\sigma_{i+1}\sigma_{i+2}\sigma_{i+3}\right],$$

where $C>0$ and E_1 are constants independent of the σ's, and E_G is the classical ground-state energy. (Here sums from i to j when $j<i$ are interpreted to be zero.) Surprisingly, there is no σ-dependent contribution at order j^4/S. This result shows that for $M>4$ second-neighboring planes are antiferromagnetically coupled in the ground state and thus the three-dimensional spin structure cannot be described by a single wave vector, as is often assumed. At order j^4, σ-dependent terms first appear at order $1/S^3$ and these also favor antiferromagnetic coupling of alternate planes.

I. INTRODUCTION

Recently there has been much attention on the phenomena of *order by disorder* in frustrated magnetic systems.[1] Thermal,[2,3] quantum,[4,5] and even quenched disorder[6] may sometimes give rise to long-range ordering in systems with frustration, where one must often consider the selection among classically degenerate ground states which are not equivalent by any symmetry. An outstanding and the simplest example is the nearest-neighbor Ising antiferromagnet (AF) on a triangular or a face-centered-cubic (fcc) lattice.[2,7,8] These systems have highly degenerate ground states. Villain *et al.* showed that at any nonzero temperature thermal fluctuations break the degeneracies in these systems, producing well-defined long-range order. They called this phenomenon ''ordering due to disorder.''[2] Later Henley[3] extended this phenomenon to a system of unit length n-component vector spins on a fcc lattice and showed that thermal fluctuations select the collinear states out of infinite degenerate ground-state manifold. At zero temperature where the thermal fluctuations are absent, ground-state selection occurs due to quantum fluctuations. This phenomenon was studied theoretically by Shender[4] and shortly thereafter confirmed experimentally by inelastic neutron scattering in some antiferromagnetic garnets.[9]

Since the work of Ref. 4, a large number of systems have been studied,[10] such as AF spins on a square and cubic lattice with nearest and next-nearest neighbor interactions,[11] AF spins on a *kagomé* lattice,[12–16] AF spins on a pyrochlore lattice,[17] and the axial next-nearest-neighbor Ising model,[18] etc. All of these studies show that ''order by disorder'' is very general in that it should exist in many quantum systems with a classically degenerate ground state. In the cases of interest to us here, it is found that quantum fluctuations favor

states in which spins are collinear. Hence, for a system where all possible collinear states are symmetry equivalent, the removal of the infinite degeneracy of the ground-state manifold by quantum fluctuations is as complete as permitted by symmetry and one has a ground state with no accidental degeneracy. To the best of our knowledge all collinear systems studied so far are of this type and hence it is of interest to study how quantum fluctuations select a unique ground state if the collinear states are not all symmetry equivalent. This issue is addressed in this paper by studying a particular system, namely quantum spins with nearest-neighbor AF interactions on a body-centered-tetragonal (bct) lattice. In this system, the Shender mechanism can only resolve the continuous degeneracy of the ground-state manifold into an infinite discrete Ising-type degeneracy, as we shortly discuss below. The selection of a unique ground state out of this infinite Ising-type degenerate manifold by higher-order effects of quantum fluctuations is analyzed in detail in this paper. Another case where collinear configurations are not equivalent by symmetry is provided by the ''second kind of AF ordering'' on an fcc lattice[19] where one has two inequivalent collinear states; type A and type B. We studied this system elsewhere[20] and found that quantum fluctuations favor the state of type A.

Three-dimensional (3D) magnetic ordering in a bct antiferromagnet is of special interest because the magnetic properties of such structures are believed to be relevant to high-temperature superconductivity. The most important example of such layered structures is perhaps La_2CuO_4,[21] in which long-range magnetic order is observed below $T_N \sim 300$ K. However it is now believed that most of the magnetic properties can be understood in terms of the Dzyaloshinskii-Moriya interaction which arises due to the orthorhombic distortion.[22] Recently, new systems which preserve the tetragonal symmetry at all temperatures have been studied. Rare-earth (R) cuprates, R_2CuO_4 (Ref. 23) (which superconduct after electron doping[24]) and $Sr_2CuO_2Cl_2$ (Ref. 25) are the most studied ones. In particular, the latter compound is the best experimental realization of the system that we are going to study in this paper. However, as we have discussed in Ref. 26, there are other type of interactions, such as the magnetic dipole interaction, magnetic anisotropy, and biquadratic exchange interactions, which may compete with the effective interactions due to quantum disorder we are going to calculate here. Accordingly, it is important calculate the effective interaction due to quantum fluctuations in order to compare its strength with that of other interactions.

We now describe in detail the model that we are going to study in this paper. We consider a bct antiferromagnet with dominant antiferromagnetic interactions between nearest neighbors in the same basal plane and weaker interactions between nearest neighbors in adjacent planes, as illustrated in Fig. 1. (The interplane interactions may be either ferromagnetic or antiferromagnetic.) From the work of Ref. 4, one may conclude that zero-point fluctuations give rise to a collinearity zero-point energy of order

$$\Delta E \sim -J_\perp^2 S[1+(\hat{n}_i \cdot \hat{n}_{i+1})^2]/J, \tag{1}$$

where J ($J_\perp$) is the antiferromagnetic coupling between nearest-neighbor spins in the same (adjacent) basal plane of the bct lattice and $\hat{n}_i$ defines the orientation of the staggered

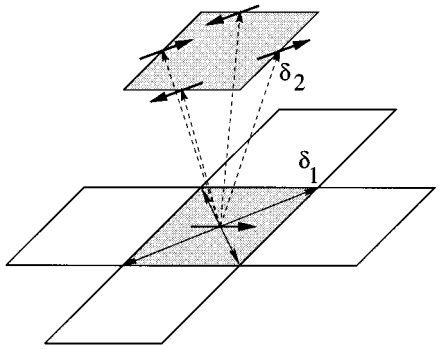

FIG. 1. A spin with its interactions. The full lines show the nearest-neighbor vectors, $\vec{\delta}_1$ in the plane for the interaction J. The dashed lines show the nearest-neighbor vectors $\vec{\delta}_2$ from the pth plane to the $p+1$st plane (above it) for the interaction $J_\perp$. Note that the mean-field interaction between adjacent planes is zero and thus the direction of the staggered magnetization in each plane is arbitrary.

magnetization in the ith plane. Thus the continuous degeneracy with respect to the orientations of the $\hat{n}$'s, is resolved into a twofold degeneracy for each collinear $\hat{n}_i$. Actually, the exact symmetry of this Heisenberg system is such that if one fixes the $\hat{n}_i$ for alternate (even-numbered, say) planes, then the configuration obtained by the replacement for all odd-numbered layers $\hat{n}_i \rightarrow -\hat{n}_i$ is degenerate in energy with the original one. This exact symmetry (due to the fourfold axes of the tetragonal crystal) indicates that there is no possibility of finding an effective interaction of the form $C\hat{n}_i \cdot \hat{n}_{i+1}$. However, symmetry *does* allow an interaction of the form $C\hat{n}_i \cdot \hat{n}_{i+2}$, which would uniquely fix the orientation of all even numbered layers with respect to one another. One should note the physical origin of these zero-point effects: although the classical ground-state energy is independent of the $\hat{n}$'s, the spin-wave spectrum does depend on these variables. Thus the quantum zero-point motion, which involves a sum over spin-wave energies, can introduce a dependence on the $\hat{n}$'s and thus lead to ground-state selection. Very simple approximate calculations of these effects are possible.[29,30] A discussion of quantum ground-state selection can be found in Ref. 1.

As far as we know, there are two studies of the effect of quantum fluctuations on the structure of the bct antiferromagnet.[27,28] On the whole, their conclusions are as expected from Ref. 4 in that collinear spin structures are favored. In contrast, some of the more detailed conclusions regarding the global spin structure of the ground state of bct antiferromagnets are less well established. For instance, Ref. 27 considered only helical configurations with particular emphasis on the structure with helical wave vector equal to $2\pi\hat{i}/a$, which we refer to as ''Case I.'' In this structure next-nearest antiferromagnetic x-y planes are stacked in phase, as is illustrated in Fig. 2. In this model adjacent x-y planes are forced to stack so as to form a helical configuration, corresponding to a single wave vector. This work did not address nonhelical stacking sequences in which successive layers have arbitrary phases. In particular ''case II,'' where next-nearest x-y planes are stacked out of phase, is not subject to a helical description. In a later work,[28] Rastelli *et al.* consid-

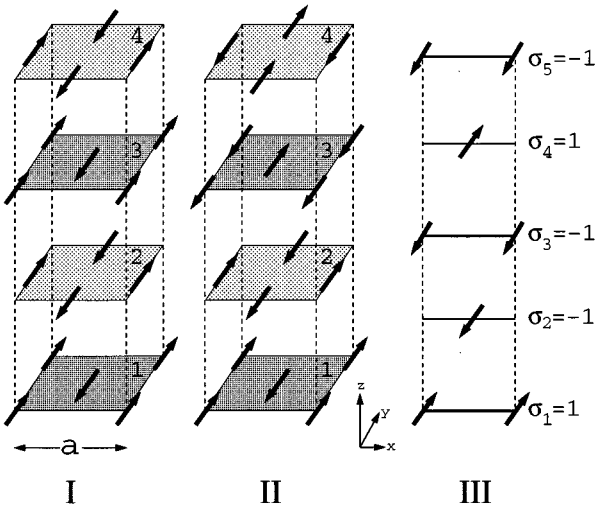

FIG. 2. Various spin structures. Structures I and II have unit cells which span two and four planes (perpendicular to $\hat{z}$), respectively. In the right-most panel, spins of an arbitrary structure (III) in the plane $y=0$ are shown. The values of σ_i for the ith plane perpendicular to $\hat{z}$ as defined by Eqs. (7) and (9), are given.

ered a less restrictive model in which even numbered planes were described by a helix with a given wave vector and initial phase angle and odd numbered planes were described by a helix with the same wave vector but with an independent initial phase angle. This formulation included more structures, and in particular it included case II of Fig. 2. Their model was more general than the one considered here in that they allowed an interaction, $J_3 \equiv j_3 J$, between nearest neighboring spins in second neighboring x-y planes. However, they stated that "for any $j_3 \leqslant 0$ the AF_1[i.e., I in Fig. 2] configuration is established." But they did not carry out any calculations for the case $j_3=0$, for which the infinite degeneracy still remains.

We have decided to reopen the study of this situation for two reasons. First of all, it appears that no comparison has actually been made between structures I and II of Fig. 2. Secondly, there still has not yet been given a treatment of arbitrary nonhelical configurations, which is the essential and correct way to treat this problem with its most general form. In order to treat arbitrary configurations we take advantage of the well established fact (which we rederive here) that zero-point fluctuations favor collinear structures.[4] The most general collinear stacking of antiferromagnetic planes is described by introducing one Ising-like variable for each plane to specify the phase of that plane. We then develop an expansion scheme in which we can calculate the zero-point energy for an arbitrary set of these Ising variables. We carry the calculations of the ground-state energy up to the order in $J_\perp/J$ at which the classical degeneracy is first removed. In that way we establish that structure II of Fig. 2 is stabilized by zero-point fluctuations, at least if one considers only effects at order $1/S$. This stabilization energy is of order $J_\perp^6 S/J^5$. Since $J_\perp/J$ can be very much smaller than $1/S$, we carried out perturbation theory in $1/S$, to locate contributions to the stabilization energy which were of order $J_\perp^4/J^3$ but were higher order in $1/S$. We found a stabilization energy of order $J_\perp^4/(J^3 S)$. As with the zero-point energy of linear spin-waves, this energy stabilizes structure II of Fig. 2.

Briefly this paper is organized as follows. In Sec. II we describe the model and discuss the expected form of the results. In Sec. III we study the effects of zero-point energy associated with noninteracting spin waves. These corrections, all of relative order $1/S$, indicate that the coupling energy between second-neighboring planes tends to set them antiparallel and, surprisingly, is of relative order j^6, where $j=J_\perp/J$. In Sec. IV we find the coupling energy for second-neighboring planes which is of order j^4. This contribution requires consideration of spin-wave interactions and is of relative order $1/S^3$. Finally our conclusions are summarized in Sec. V.

II. FORMALISM

A. Statement of the model

We consider $M\times(2N)$ spins on the sites of a bct lattice consisting of M 2D antiferromagnetic layers, each consisting of $2N$ strongly coupled antiferromagnetic spins on a square lattice with periodic boundary conditions. We write the Hamiltonian as

$$\mathscr{H}=\sum_{p=1}^{M} H_p+\sum_{p=1}^{M-1} H_{p,p+1}, \tag{2}$$

where H_p refers to the pth plane alone and is given by

$$H_p=J\sum_{i,\delta_1} \mathbf{S}_p(\mathbf{r}_i)\cdot\mathbf{S}_p(\mathbf{r}_i+\delta_1) \tag{3}$$

and the interaction $H_{p,p+1}$ between the pth and $(p+1)$th planes is

$$H_{p,p+1}=2J_\perp\sum_{i,\delta_2} \mathbf{S}_p(\mathbf{r}_i)\cdot\mathbf{S}_{p+1}(\mathbf{r}_i+\delta_2), \tag{4}$$

where $\mathbf{S}_p(\mathbf{r}_i)$ is the spin at position $\mathbf{r}_i$ in plane p. Also δ_1 and δ_2 are the vectors joining a site to its NN's in plane and NN's out of plane, respectively, as shown in Fig. 1. We find it convenient to describe each antiferromagnetic layer in terms of a Bravais lattice with a two-spin basis. Thus up spins in an odd-numbered layer (p) have

$$\mathbf{r}_i=(n_1\hat{i}+n_2\hat{j})a+\tau_1(\mathbf{p}) \tag{5}$$

and down spins in odd-numbered layers have

$$\mathbf{r}_i=(n_1\hat{i}+n_2\hat{j})a+\tau_2(p), \tag{6}$$

where

$$\tau_1(p)=(1-\sigma_p)(\hat{i}+\hat{j})a/4 \tag{7}$$

and

$$\tau_2(p)=(1+\sigma_p)(\hat{i}+\hat{j})a/4. \tag{8}$$

Here a is a lattice constant and $\hat{i}$ ($\hat{j}$) is a unit vector in the basal plane along the x (y) direction. The meaning of Eq. (7) is that if $\sigma_p=1$ (for odd p), the spin at the origin is up and if

$\sigma_p=-1$, it is down. For an even-numbered plane (p) we still have Eqs. (5) and (6) for up and down spins, respectively, but for this case

$$\tau_1(p)=(\hat{i}+\hat{j})a/4+\sigma_p(\hat{i}-\hat{j})a/4 \tag{9}$$

and

$$\tau_2(p)=(\hat{i}+\hat{j})a/4-\sigma_p(\hat{i}-\hat{j})a/4. \tag{10}$$

Thus for p even, $\sigma_p=1$ means that the spin at $x=a/2$, $y=0$ in the pth plane is up. These parametrizations are illustrated in Fig. 2.

B. Transformation to bosons

We introduce the transformation to bosons in the usual way,[31] according to the Dyson-Maleev transformation.[32] For up spins we write

$$S_p^z(i)=S-a^+(p;i)a(p;i), \tag{11}$$

$$S_p^+(i)=\sqrt{2S}[1-a^+(p;i)a(p;i)/(2S)]a(p;i), \tag{12}$$

$$S_p^-(i)=\sqrt{2S}a^+(p;i), \tag{13}$$

and for down spins

$$S_p^z(i)=-S+b^+(p;i)b(p;i), \tag{14}$$

$$S_p^+(i)=\sqrt{2S}b^+(p;i)[1-b^+(p;i)b(p;i)/(2S)], \tag{15}$$

$$S_p^-(i)=\sqrt{2S}b(p;i). \tag{16}$$

Here we should note that the form of the interaction depends on whether the interacting spins are parallel or are antiparallel. However, changing the interplanar interactions from antiferromagnetic to ferromagnetic only involves changing the sign of $J_\perp$. Hence all our results will be valid for either sign of $J_\perp$. In fact, to lowest order in $J_\perp$ we will see that the results do not depend on the sign of this variable.

Fourier transformed variables are defined by

$$a^+(p;i)=\frac{1}{\sqrt{N}}\sum_{\mathbf{q}} e^{i\mathbf{q}\cdot\mathbf{r}_i}a_p^+(\mathbf{q}), \tag{17}$$

$$b^+(p;i)=\frac{1}{\sqrt{N}}\sum_{\mathbf{q}} e^{i\mathbf{q}\cdot\mathbf{r}_i}b_p^+(\mathbf{q}),$$

where the sum is over the N wave vectors in the magnetic Brillouin zone: $|q_x|<\pi/a$ and $|q_y|<\pi/a$. Note that in each plane there are $2N$ spins and $\mathbf{r}_i$ is a vector in the x-y plane. The Hamiltonian in Eq. (2) can be written in momentum space as

$$\mathscr{H}=E_G+\sum_{p=1}^{M} H_p^{(2)}+\sum_{p=1}^{M-1} V(p,p+1)+\sum_{p=1}^{M} H_p^{(4)}+\sum_{p=1}^{M-1} H_{p,p+1}^{(4)}. \tag{18}$$

Here $E_G=-2MNzJS^2$ is the classical ground-state energy, where $z=4$ is the coordination number within a layer, $H_p^{(2)}$ and $V(p,p+1)$ represent the interactions quadratic in boson operators, respectively, within the pth layer and between layers p and $p+1$, and $H_p^{(4)}$ and $H_{p,p+1}^{(4)}$ are the analogous interactions quartic in boson operators.

We have

$$H_p^{(2)}=2zJS\sum_{\mathbf{q}} \{a_p^+(\mathbf{q})a_p(\mathbf{q})+b_p^+(\mathbf{q})b_p(\mathbf{q})+\gamma_{\mathbf{q}}[a_p(\mathbf{q})b_p(-\mathbf{q})+a_p^+(\mathbf{q})b_p^+(-\mathbf{q})]\}, \tag{19}$$

where

$$\gamma_{\mathbf{q}}=z^{-1}\sum_{\delta_1} e^{i\mathbf{q}\cdot\delta_1}=\cos(q_xa/2)\cos(q_ya/2). \tag{20}$$

To obtain $V(p,p+1)$ we write[33]

$$V(p,p+1)=2J_\perp S\sum_{ij} \{[a^+(p;i)a(p+1;j)+b^+(p;i)b(p+1;j)]\gamma_{p,p+1}^{(L)}(i,j)+[a(p;i)b(p+1;j)+b(p;j)a(p+1;i)]\gamma_{p,p+1}^{(U)}(i,j)+\text{H.c.}\}, \tag{21}$$

where $\gamma_{p,p+1}^{(L)}(i,j)$ is unity if spins i in plane p and j in plane $p+1$ are like (i.e., either both up or both down) and are nearest interplanar neighbors and is zero otherwise, $\gamma_{p,p+1}^{(U)}(i,j)$ is unity if spins i and j are unlike (i.e., one up and one down) and are nearest interplanar neighbors and is zero otherwise, and H.c. indicates the Hermitian conjugate of all the preceding terms inside the bracket. Thus

$$V(p,p+1)=4J_\perp S\sum_{\mathbf{q}} \{\gamma_{p,p+1}^{(L)}(\mathbf{q})[a_p^+(\mathbf{q})a_{p+1}(\mathbf{q})+b_p^+(\mathbf{q})b_{p+1}(\mathbf{q})]+\gamma_{p,p+1}^{(U)}(\mathbf{q})[a_p(\mathbf{q})b_{p+1}(-\mathbf{q})+b_p(\mathbf{q})a_{p+1}(-\mathbf{q})]\}+\text{H.c.}, \tag{22}$$

where we have the Fourier transforms

$$\gamma_{p,p+1}^{(L)}(\mathbf{q})=c_{\mathbf{q}}-\sigma_{p,p+1}s_{\mathbf{q}}, \quad \gamma_{p,p+1}^{(U)}(\mathbf{q})=c_{\mathbf{q}}+\sigma_{p,p+1}s_{\mathbf{q}}, \tag{23}$$

where

$$c_{\mathbf{q}}=\cos[a(q_x+q_y)/4]\cos[a(q_x-q_y)/4], \quad s_{\mathbf{q}}=\sin[a(q_x+q_y)/4]\sin[a(q_x-q_y)/4], \tag{24}$$

and $\sigma_{p,p+1}=\sigma_p\sigma_{p+1}$. Useful relations involving $c_{\mathbf{q}}$ and $s_{\mathbf{q}}$ are developed in Appendix C of Ref. 34. Also $H_p^{(4)}$ is the quartic part of the term describing the pth plane alone and is given by

$$H_p^{(4)}=-\frac{Jz}{N}\sum_{1,2,3,4,\mathbf{G}} e^{i\mathbf{G}\cdot\tau_1(p)}\delta_{\mathbf{G}}[2a_p^+(1)a_p(-2)b_p^+(3)b_p(-4)\gamma_{3+4}$$
$$+a_p^+(1)a_p(-2)a_p^+(3)b_p(-4)\gamma_4+a_p^+(1)b_p^+(2)b_p^+(3)b_p(-4)\gamma_{2+3+4}], \tag{25}$$

where $\delta_{\mathbf{G}}=\delta(1+2+3+4+\mathbf{G})$, $1\equiv\mathbf{q}_1$, $2\equiv\mathbf{q}_2$, etc., the wave vectors are all summed over the magnetic Brillouin zone, and $\mathbf{G}$ is summed over all reciprocal-lattice vectors: $\mathbf{G}=(n_1\hat{i}+n_2\hat{j})(2\pi/a)$. The occurrence of the phase factor in Eq. (25) may not be familiar, so we discuss it in Appendix A. In carrying out a calculation for a single plane, these phase factors never have any significance (because they depend on the absolute placement of the origin), but here we must keep track of them (because the location of the origin of one plane relative to that of a neighboring plane is significant).

Also $H_{p,p+1}^{(4)}$, the quartic part of the term describing the interaction between planes p and $p+1$ is given by

$$H_{p,p+1}^{(4)}=V_{zz}(p,p+1)+V_{\mathrm{NL}}(p,p+1)+V_{\mathrm{NL}}(p+1,p), \tag{26}$$

where the terms come from the S_zS_z, S_+S_-, and S_-S_+ interactions, respectively. Then

$$V_{zz}(p,p+1)=\frac{4J_\perp}{N}\sum_{1,2,3,4\mathbf{G}}\delta_{\mathbf{G}}e^{i\mathbf{G}\cdot\tau_1(p)}\{a_p^+(1)a_p(-2)[\gamma_{p,p+1}^{(L)}(3+4)a_{p+1}^+(3)a_{p+1}(-4)-\gamma_{p,p+1}^{(U)}(3+4)b_{p+1}^+(3)b_{p+1}(-4)]$$
$$\times b_p^+(1)b_p(-2)[\gamma_{p,p+1}^{(L)}(3+4)b_{p+1}^+(3)b_{p+1}(-4)-\gamma_{p,p+1}^{(U)}(3+4)a_{p+1}^+(3)a_{p+1}(-4)]\gamma_{\mathbf{G}}\}, \tag{27}$$

$$V_{\mathrm{NL}}(p+1,p)=-\frac{2J_\perp}{N}\sum_{1234,\mathbf{G}}\delta_{\mathbf{G}}e^{i\mathbf{G}\cdot\tau_1(p)}$$
$$\times\{[a_p^+(1)\gamma_{p,p+1}^{(L)}(2+3+4)+\gamma_{\mathbf{G}}b_p(-1)\gamma_{p,p+1}^{(U)}(2+3+4)]a_{p+1}^+(2)a_{p+1}(-3)a_{p+1}(-4)$$
$$+[a_p^+(1)\gamma_{p,p+1}^{(U)}(2+3+4)+\gamma_{\mathbf{G}}b_p(-1)\gamma_{p,p+1}^{(L)}(2+3+4)]b_{p+1}^+(2)b_{p+1}^+(3)b_{p+1}(-4)\}, \tag{28}$$

and $V_{\mathrm{NL}}(p,p+1)$ is obtained from $V_{\mathrm{NL}}(p+1,p)$ by interchanging the roles of p and $p+1$. Equation (28) is discussed in Appendix A.

We now introduce a Bogoliubov transformation to diagonalize $H_p^{(2)}$

$$a_p(\mathbf{q})^+=l_{\mathbf{q}}\alpha_p^+(\mathbf{q})-m_{\mathbf{q}}\beta_p(-\mathbf{q});$$
$$b_p(-\mathbf{q})=-m_{\mathbf{q}}\alpha_p^+(\mathbf{q})+l_{\mathbf{q}}\beta_p(-\mathbf{q}), \tag{29}$$

where

$$l_{\mathbf{q}}=\sqrt{\frac{1+\epsilon_{\mathbf{q}}}{2\epsilon_{\mathbf{q}}}}, \quad m_{\mathbf{q}}=\sqrt{\frac{1-\epsilon_{\mathbf{q}}}{2\epsilon_{\mathbf{q}}}}, \quad \epsilon_{\mathbf{q}}=\sqrt{1-\gamma_{\mathbf{q}}^2}. \tag{30}$$

Then we rewrite the Hamiltonian in terms of magnon operators as

$$\mathscr{H}=E_G'+\sum_{p=1}^{M}H_p'^{(2)}+\sum_{p=1}^{M-1}H_{p,p+1}'^{(2)}+\sum_{p=1}^{M}H_p'^{(4)}$$
$$+\sum_{p=1}^{M-1}H_{p,p+1}'^{(4)}, \tag{31}$$

where

$$E_G'=-2NMzJS^2[1+\xi/S]^2, \tag{32}$$

with

$$\xi=N^{-1}\sum_{\mathbf{q}}(1-\epsilon_{\mathbf{q}})/2. \tag{33}$$

The presence of the factor ξ comes from reordering operators so that creation operators are to the left of annihilation operators. In other words, ξ indicates corrections due to quantum zero-point motion. However, since these corrections are all intraplane corrections, they do not affect our calculation in a significant way. As we will see, they simply rescale S and J in an inessential way.

The quadratic part of the term describing pth plane alone is

$$H_p'^{(2)}=2z\tilde{J}S\sum_{\mathbf{q}}\epsilon_{\mathbf{q}}[\alpha_p^+(\mathbf{q})\alpha_p(\mathbf{q})+\beta_p^+(\mathbf{q})\beta_p(\mathbf{q})], \tag{34}$$

where $\tilde{J}=J[1+\xi/S]$ includes the effects of normally ordering $H_p^{(4)}$.

The quadratic part of the term describing the interaction between planes p and $p+1$ is

$$H'^{(2)}_{p,p+1}=4J_\perp\tilde{S}\sum_{\mathbf{q}}\{X_{p,p+1}(\mathbf{q})[\alpha^+_p(\mathbf{q})\alpha_{p+1}(\mathbf{q})+\beta^+_p(\mathbf{q})\beta_{p+1}(\mathbf{q})]+Y_{p,p+1}(\mathbf{q})[\alpha_p(\mathbf{q})\beta_{p+1}(-\mathbf{q})+\beta_p(\mathbf{q})\alpha_{p+1}(-\mathbf{q})]\}+\text{H.c.},\tag{35}$$

where $\tilde{S}=S-N^{-1}\Sigma_{\mathbf{q}}m_q^2$ includes the effects of normally ordering $H^{(4)}_{p,p+1}$, and

$$X_{p,p+1}(\mathbf{q})=\gamma^{(L)}_{p,p+1}(\mathbf{q})(l^2_{\mathbf{q}}+m^2_{\mathbf{q}})-2l_{\mathbf{q}}m_{\mathbf{q}}\gamma^{(U)}_{p,p+1}(\mathbf{q})=t_c(\mathbf{q})-\sigma_{p,p+1}t_s(\mathbf{q}),\tag{36}$$

$$Y_{p,p+1}(\mathbf{q})=\gamma^{(U)}_{p,p+1}(\mathbf{q})(l^2_{\mathbf{q}}+m^2_{\mathbf{q}})-2l_{\mathbf{q}}m_{\mathbf{q}}\gamma^{(L)}_{p,p+1}(\mathbf{q})=t_c(\mathbf{q})+\sigma_{p,p+1}t_s(\mathbf{q}),\tag{37}$$

where

$$t_c(\mathbf{q})=\left(\frac{1-\gamma_{\mathbf{q}}}{\epsilon_{\mathbf{q}}}\right)\cos[a(q_x+q_y)/4]\cos[a(q_x-q_y)/4],\tag{38}$$

$$t_s(\mathbf{q})=\left(\frac{1+\gamma_{\mathbf{q}}}{\epsilon_{\mathbf{q}}}\right)\sin[a(q_x+q_y)/4]\sin[a(q_x-q_y)/4].\tag{39}$$

The explicit expressions for the quartic part of the Hamiltonian in terms of normal-mode operators will be given in Sec. IV when we calculate the contributions at higher order of $1/S$.

C. Perturbation theory in 1/S and $J_\perp$

We may write the quantum corrections to the ground-state energy as

$$\Delta E=E-E_G=E_G\sum_{n,m}a_{nm}(j)^n(1/S)^m\equiv E_Ge,\tag{40}$$

where $j=J_\perp/J$. Shender's[4] result that the zero-point energy favors collinearity is contained in the term a_{21}, as already mentioned in Eq. (1) and implicitly assumed by the form of the transformation to bosons. If we evaluate the zero-point energy in terms of the sum over all spin-wave modes of the 3D system, we will get all contributions to e of order $1/S$. We will carry out such a calculation only to an order in j sufficient to obtain a dependence on the σ's. As we shall see, this requires an evaluation of all terms of order $1/S$ up to and including order j^6. It is somewhat surprising that to get a coupling between second-neighboring planes at order $1/S$ one has to go to order j^6. In fact, if the calculations are extended to higher order in $1/S$, we expect to eventually get a contribution to e of order j^4 which does depend on the σ's. This calculation, requiring an evaluation of e up to order $1/S^3$ is described in Sec. IV.

III. 1/S CALCULATION

We show here how the contributions to the quantum zero-point energy can be calculated to arbitrary order in j at first order in $1/S$ for an arbitrary configuration of σ's. Such a calculation seemingly requires a calculation of the normal modes of such a nonuniform system. Obviously, an exact calculation of the normal modes is out of the question. We start by noting from Eq. (34) that the Hamiltonian quadratic in the normal modes can be written in the form

$$\mathscr{H}_2=\sum_{\mathbf{q}}\mathscr{H}_2(\mathbf{q}),\tag{41}$$

where $\mathscr{H}_2(\mathbf{q})$ is a product of matrices of the form

$$\mathscr{H}_2(\mathbf{q})=\sum_{\mathbf{q}}[X^+HX-ME_0(\mathbf{q})],\tag{42}$$

where $E_0(\mathbf{q})=2z\tilde{J}S\epsilon_{\mathbf{q}}$, X is a column matrix with elements taken from the operators which appear in the Hamiltonian, and H is a $2M\times 2M$ square matrix formed with the coefficients of the Hamiltonian, i.e.,

$$X=\begin{pmatrix}\alpha^+_1(\mathbf{q})\\ \vdots\\ \alpha^+_M(\mathbf{q})\\ \beta_1(-\mathbf{q})\\ \vdots\\ \beta_M(-\mathbf{q})\end{pmatrix},\quad H=\begin{pmatrix}H_1(\mathbf{q}) & H_2(\mathbf{q})\\ H_2(\mathbf{q}) & H_1(\mathbf{q})\end{pmatrix}_{2M\times 2M}\tag{43}$$

where

$$H_1=\begin{pmatrix}E_0(\mathbf{q}) & K_1(\mathbf{q}) & & & & & \\ K_1(\mathbf{q}) & E_0(\mathbf{q}) & K_2(\mathbf{q}) & & & & \\ & K_2(\mathbf{q}) & E_0(\mathbf{q}) & K_3(\mathbf{q}) & & & \\ & & \ddots & \ddots & \ddots & & \\ & & & K_{M-2}(\mathbf{q}) & E_0(\mathbf{q}) & K_{M-1}(\mathbf{q}) \\ & & & & K_{M-1}(\mathbf{q}) & E_0(\mathbf{q})\end{pmatrix}\tag{44}$$

and

$$H_2=\begin{pmatrix} 0 & L_1(\mathbf{q}) & & & & & \\ L_1(\mathbf{q}) & 0 & L_2(\mathbf{q}) & & & & \\ & L_2(\mathbf{q}) & 0 & L_3(\mathbf{q}) & & & \\ & & \ddots & \ddots & \ddots & & \\ & & & L_{M-2}(\mathbf{q}) & 0 & L_{M-1}(\mathbf{q}) & \\ & & & & L_{M-1}(\mathbf{q}) & 0 & \end{pmatrix}, \tag{45}$$

in the above matrices the entries which are not shown are all zero, and

$$K_p(\mathbf{q})=4J_\perp\tilde{S}X_{p,p+1}(\mathbf{q}), \tag{46}$$

$$L_p(\mathbf{q})=4J_\perp\tilde{S}Y_{p,p+1}(\mathbf{q}). \tag{47}$$

The square of the spin-wave energies of the Hamiltonian in Eq. (42) are the eigenvalues of the dynamical matrix

$$H_{+-}=H_+H_-, \tag{48}$$

where

$$H_+=H_1+H_2=E_0(\mathbf{q})\begin{pmatrix} 1 & \tilde{j}p(\mathbf{q}) & & & & & \\ \tilde{j}p(\mathbf{q}) & 1 & \tilde{j}p(\mathbf{q}) & & & & \\ & \tilde{j}p(\mathbf{q}) & 1 & \tilde{j}p(\mathbf{q}) & & & \\ & & \ddots & \ddots & \ddots & & \\ & & & \tilde{j}p(\mathbf{q}) & 1 & \tilde{j}p(\mathbf{q}) & \\ & & & & \tilde{j}p(\mathbf{q}) & 1 & \end{pmatrix}\equiv E_0(\mathbf{q})[\mathbf{I}+\tilde{j}p(\mathbf{q})\Lambda_1] \tag{49}$$

and

$$H_-=H_1-H_2=E_0(\mathbf{q})\begin{pmatrix} 1 & \tilde{j}r_1 & & & & \\ \tilde{j}r_1 & 1 & \tilde{j}r_2 & & & \\ & \tilde{j}r_2 & 1 & \tilde{j}r_3 & & \\ & & \ddots & \ddots & \ddots & \\ & & & \tilde{j}r_{M-2} & 1 & \tilde{j}r_{M-1} \\ & & & & \tilde{j}r_{M-1} & 1 \end{pmatrix}\equiv E_0(\mathbf{q})[\mathbf{I}+\tilde{j}r(\mathbf{q})\Lambda_2]. \tag{50}$$

$\mathbf{I}$ is the unit matrix, $\tilde{j}=J_\perp\tilde{S}/(\tilde{J}S)$, and

$$p(\mathbf{q})=\frac{t_c(\mathbf{q})}{\epsilon_\mathbf{q}}=\frac{1}{1+\gamma_\mathbf{q}}\cos[a(q_x+q_y)/4]\cos[a(q_x-q_y)/4], \tag{51}$$

$$r_i=-\frac{t_s(\mathbf{q})}{\epsilon_\mathbf{q}}\sigma_i\sigma_{i+1}=-\frac{\sigma_i\sigma_{i+1}}{1-\gamma_\mathbf{q}}\sin\left(\frac{a}{4}(q_x+q_y)\right)\sin\left(\frac{a}{4}(q_x-q_y)\right)\equiv r(\mathbf{q})\sigma_i\sigma_{i+1}, \tag{52}$$

and

$$\Lambda_1=\begin{pmatrix} 0 & 1 & & & & \\ 1 & 0 & 1 & & & \\ & 1 & 0 & 1 & & \\ & & \ddots & \ddots & \ddots & \\ & & & 1 & 0 & 1 \\ & & & & 1 & 0 \end{pmatrix},\quad \Lambda_2=\begin{pmatrix} 0 & \sigma_1\sigma_2 & & & & \\ \sigma_1\sigma_2 & 0 & \sigma_2\sigma_3 & & & \\ & \sigma_2\sigma_3 & 0 & \sigma_3\sigma_4 & & \\ & & \ddots & \ddots & \ddots & \\ & & & \sigma_{M-2}\sigma_{M-1} & 0 & \sigma_{M-1}\sigma_M \\ & & & & \sigma_{M-1}\sigma_M & 0 \end{pmatrix}. \tag{53}$$

The eigenvalues $E_i(\mathbf{q})$ are the solutions of the characteristic equation

$$F(E_i)=\det[x_i^2(\mathbf{q})\mathbf{I}-\tilde{j}p(\mathbf{q})\Lambda_1-\tilde{j}r(\mathbf{q})\Lambda_2 -\tilde{j}^2p(\mathbf{q})r(\mathbf{q})\Lambda_1\Lambda_2]=0, \tag{54}$$

where $x_i^2(\mathbf{q})=[E_i(\mathbf{q})/E_0(\mathbf{q})]^2-1$. After normal ordering of operators, one finds

$$\mathscr{H}_2=\Delta E_Q+\sum_{i=1}^{M}\sum_{\mathbf{q}} E_i(\mathbf{q})[\eta_i^+(\mathbf{q})\eta_i(\mathbf{q})+\rho_i^+(\mathbf{q})\rho_i(\mathbf{q})], \tag{55}$$

where the η's and ρ's are the exact normal modes of the M-layer system and ΔE_Q is given by

$$\Delta E_Q=\sum_{\mathbf{q}}\sum_{i=1}^{M}[E_i(\mathbf{q})-E_0(\mathbf{q})]\equiv(2NJzS^2)\Delta e_Q, \tag{56}$$

where Δe_Q is normalized relative to the classical energy per plane and

$$E_i(\mathbf{q})=E_0(\mathbf{q})\sqrt{1+x_i^2(\mathbf{q})}. \tag{57}$$

Since $F(E_i)$ given in Eq. (54) is of high degree, it cannot be solved explicitly. However, to calculate the quantum correction in ΔE_Q to any finite order of j we need, not the roots $x_i(\mathbf{q})$, but only the *summation of any power of them*. We can see this by writing Δe_Q as

$$\Delta e_Q=S^{-1}\sum_{i=1}^{M}N^{-1}\sum_{q}\epsilon_{\mathbf{q}}[\sqrt{1+x_i^2(\mathbf{q})}-1] \tag{58}$$

and then expanding in powers of $x_i^2(\mathbf{q})$ to get

$$\Delta e_Q=S^{-1}\sum_{m=0}^{\infty}k_mN^{-1}\sum_{\mathbf{q}}\epsilon_{\mathbf{q}}\mathrm{Tr}[\tilde{j}p(\mathbf{q})\Lambda_1+\tilde{j}r(\mathbf{q})\Lambda_2 +\tilde{j}^2p(\mathbf{q})r(\mathbf{q})\Lambda_1\Lambda_2]^m, \tag{59}$$

where

$$k_m=(-1)^{m-1}\frac{(2m)!}{2^{2m}(m!)^2(2m-1)}. \tag{60}$$

Note that the term with $m=0$ corresponds to the case where the planes do not couple with each other and hence the total quantum correction is just the number of planes times the quantum correction due to a single plane. In this expansion we find the desired dependence on the σ's at order $\tilde{j}^6$. To evaluate terms in Eq. (59) we note that only terms in which Λ_1 and Λ_2 both appear an even number of terms survive the trace and integration over $\mathbf{q}$. For such terms we needed to use (for $M>2$)

$$\mathrm{Tr}\Lambda_1^2=\mathrm{Tr}\Lambda_2^2=2M-2,$$

$$\mathrm{Tr}\Lambda_1^4=\mathrm{Tr}\Lambda_2^4=6M-10,$$

$$\mathrm{Tr}\Lambda_1^6=\mathrm{Tr}\Lambda_2^6=20M-44,$$

$$\mathrm{Tr}[2\Lambda_1^2\Lambda_2^2-\Lambda_1\Lambda_2\Lambda_1\Lambda_2]=6M-10,$$

$$\mathrm{Tr}[14\Lambda_1^4\Lambda_2^2-6\Lambda_2\Lambda_1\Lambda_2\Lambda_1^3-3\Lambda_1^2\Lambda_2\Lambda_1^2\Lambda_2] =27M-57-4\sigma_1\sigma_3-4\sigma_{M-2}\sigma_M+4\sum_{j=1}^{M-2}\sigma_j\sigma_{j+2} -6\sum_{j=1}^{M-3}\sigma_j\sigma_{j+1}\sigma_{j+2}\sigma_{j+3}. \tag{61}$$

In the last equation, the four-spin term is absent for $M=3$. Thereby we finally obtain the result

$$\Delta e_Q=\frac{2}{S}\left[-\frac{M-1}{8}I_2j^2+\left(\frac{(3M-5)}{2^6}I_{22}-\frac{5(3M-5)}{2^7}I_4\right)j^4+\left\{\frac{27M-57}{2^9}I_{42}-\frac{105M-55}{2^9}I_6 +\frac{1}{2^9}I_{42}\left(-4\sigma_1\sigma_3-4\sigma_{M-2}\sigma_M+4\sum_{i=1}^{M-2}\sigma_i\sigma_{i+2}-6(\sigma_1\sigma_2\sigma_3\sigma_4+\cdots+\sigma_{M-3}\sigma_{M-2}\sigma_{M-1}\sigma_M)\right)\right\}j^6\right], \tag{62}$$

where the positive constants are

$$I_m=\langle p^m+r^m\rangle_{\mathbf{q}},\quad I_{2,2}=\langle p^2r^2\rangle_{\mathbf{q}},$$

$$I_{4,2}=\langle p^4r^2+r^4p^2\rangle_{\mathbf{q}}, \tag{63}$$

where

$$\langle p^mr^n\rangle_{\mathbf{q}}=N^{-1}\sum_{\mathbf{q}}p(\mathbf{q})^mr(\mathbf{q})^n\epsilon_{\mathbf{q}}. \tag{64}$$

The consequences of this result depend on the number of planes M in the system. If $M=3$, the σ-dependent part of the energy is proportional to $-\sigma_1\sigma_3$, which indicates that in this case, planes 1 and 3 have lower energy when ferromagnetically coupled. For $M=4$, the energy is proportional to

$-\sigma_1\sigma_2\sigma_3\sigma_4$. To this order the configuration of the layers still has some degeneracy and a full solution for the ground state would require evaluation of terms still higher order in j than we have here. For $M>4$, the energy is minimized when second-neighboring planes are antiparallel to one another: $\sigma_i=-\sigma_{i+2}$.

We now discuss briefly this result in the light of Refs. 27 and 28 for the case when $j_3=0$. The structure we find is the one they call AF providing their angle θ is fixed to be 90° so as to obtain a collinear structure. In principle, by comparing the spin-wave zero-point energy of this structure with that of the one (AF_1= structure I of Fig. 2) they find to be stabilized, one could verify our results. However, the procedure we follow is more general, more direct, and actually is much simpler computationally. In addition, we determine that the zero-point energy is proportional to $J_\perp^6$. As we have said, this result motivates us to analyze spin-wave interactions to locate a stabilization energy which, although higher order in $1/S$, is lower order in $J_\perp/J$. This analysis is relevant because in many cases $J_\perp/J$ is much smaller than $1/S$.

IV. EFFECTS OF SPIN-WAVE INTERACTIONS

In this section we consider the effect of spin-wave interactions, because we expect that these will give rise to a nonzero contribution to the σ-dependent energy at order j^4. To start we record the form of the quartic interactions. The quartic interaction $H_{\rm DM}$ within a single layer is obtained from Eq. (25) in terms of normal-mode operators as (with the layer subscript p on the operators omitted)

$$\begin{aligned}H_{\rm DM}(p)=&-\frac{H_E}{4NS}\sum_{1,2,3,4,\mathbf{G}}\delta_{\mathbf{G}}l_1l_2l_3l_4e^{i\mathbf{G}\cdot\tau_1(p)}[\Phi^{(1)}_{1234}\alpha^+(1)\alpha^+(2)\alpha(-3)\alpha(-4)\\&+2\Phi^{(2)}_{1234}\alpha^+(1)\beta(-2)\alpha(-3)\alpha(-4)+2\Phi^{(3)}_{1234}\alpha^+(1)\alpha^+(2)\beta^+(4)\alpha(-3)\\&+4\Phi^{(4)}_{1234}\alpha^+(1)\beta^+(4)\beta(-2)\alpha(-3)+2\Phi^{(5)}_{1234}\beta^+(3)\beta(-1)\beta(-2)\alpha(-4)\\&+2\Phi^{(6)}_{1234}\alpha^+(2)\beta^+(3)\beta^+(4)\beta(-1)+\Phi^{(7)}_{1234}\alpha^+(1)\alpha^+(2)\beta^+(3)\beta^+(4)\\&+\Phi^{(8)}_{1234}\beta(-1)\beta(-2)\alpha(-3)\alpha(-4)+\Phi^{(9)}_{1234}\beta^+(3)\beta^+(4)\beta(-1)\beta(-2)].\end{aligned}\tag{65}$$

Here

$$\begin{aligned}\Phi^{(7)}_{1234}=\gamma_{\mathbf{G}}\Phi^{(8)}_{1234}=&\gamma_{2+4}x_2x_3+\gamma_{2+3}x_2x_4+\gamma_{1+3}x_1x_4+\gamma_{1+4}x_1x_3\\&-\gamma_2x_2x_3x_4-\gamma_1x_1x_3x_4-\gamma_{1+3+4}x_1-\gamma_{2+3+4}x_2,\end{aligned}\tag{66}$$

$$\begin{aligned}\Phi^{(3)}_{1234}=\gamma_{\mathbf{G}}\Phi^{(5)}_{1234}=&-\gamma_{2+4}x_2-\gamma_{1+4}x_1-\gamma_{2+3}x_2x_3x_4-\gamma_{1+3}x_1x_3x_4\\&+\gamma_2x_2x_4+\gamma_1x_1x_4+\gamma_{2+3+4}x_2x_3+\gamma_{1+3+4}x_1x_3,\end{aligned}\tag{67}$$

$$\begin{aligned}\Phi^{(2)}_{1234}=\gamma_{\mathbf{G}}\Phi^{(6)}_{1234}=&-\gamma_{2+4}x_4-\gamma_{2+3}x_3-\gamma_{1+4}x_1x_2x_4-\gamma_{1+3}x_1x_2x_3\\&+\gamma_2+\gamma_1x_1x_2+\gamma_{2+3+4}x_3x_4+\gamma_{1+3+4}x_1x_2x_3x_4,\end{aligned}\tag{68}$$

$$\begin{aligned}\Phi^{(1)}_{1234}=\gamma_{\mathbf{G}}\Phi^{(9)}_{1234}=&\gamma_{2+4}x_2x_4+\gamma_{2+3}x_2x_3+\gamma_{1+3}x_1x_3+\gamma_{1+4}x_1x_4\\&-\gamma_2x_2-\gamma_1x_1-\gamma_{1+3+4}x_1x_3x_4-\gamma_{2+3+4}x_2x_3x_4,\end{aligned}\tag{69}$$

$$\begin{aligned}\Phi^{(4)}_{1234}=\gamma_{\mathbf{G}}\Phi^{(4)}_{2143}=&\gamma_{2+4}+\gamma_{2+3}x_3x_4+\gamma_{1+3}x_1x_2x_3x_4+\gamma_{1+4}x_1x_2\\&-\gamma_2x_4-\gamma_1x_1x_2x_4-\gamma_{1+3+4}x_1x_2x_3-\gamma_{2+3+4}x_3,\end{aligned}\tag{70}$$

where $x_i=m_i/l_i=m(\mathbf{q}_i)/l(\mathbf{q}_i)$. We have corrected the results of Ref. 31 to treat umklapp processes properly.

Now we consider the nonlinear interactions between layers. First we write down the quartic terms coming from the S_zS_z interactions. They will later be shown not to contribute at the order in $1/S$ to which we work. We have

$$\begin{aligned}V_{zz}(p,p+1)=&\frac{4J_\perp}{N}\sum_{1,2,3,4,\mathbf{G}}\delta_{\mathbf{G}}l_1l_2l_3l_4e^{i\mathbf{G}\cdot\tau_1(p)}[H^{(1)}_{1234}\alpha^+_p(1)\beta^+_p(2)\alpha^+_{p+1}(3)\beta^+_{p+1}(4)\\&+H^{(2)}_{1234}\alpha^+_p(1)\beta^+_p(2)\alpha^+_{p+1}(3)\alpha_{p+1}(-4)+H^{(3)}_{1234}\alpha^+_p(1)\beta^+_p(2)\beta^+_{p+1}(4)\beta_{p+1}(-3)+\dots].\end{aligned}\tag{71}$$

We only wrote those terms in Eq. (71) which affect our calculation. Note from Eq. (27) that V_{zz} is Hermitian. Here

$$H^{(1)}_{1234}=(x_2-x_1\gamma_{\mathbf{G}})(x_4-x_3)c_{3+4}-\sigma_p\sigma_{p+1}(x_2+x_1\gamma_{\mathbf{G}})(x_4+x_3)s_{(3+4)},\tag{72}$$

$$H^{(2)}_{1234}=(x_2-x_1\gamma_{\mathbf{G}})(x_3x_4-1)c_{3+4}+\sigma_p\sigma_{p+1}(x_2+x_1\gamma_{\mathbf{G}})(x_3x_4+1)s_{3+4},\tag{73}$$

$$H^{(3)}_{1234}=(x_2-x_1\gamma_{\mathbf{G}})(1-x_3x_4)c_{3+4}+\sigma_p\sigma_{p+1}(x_2+x_1\gamma_{\mathbf{G}})(1+x_3x_4)s_{3+4}. \tag{74}$$

The quartic perturbations from the transverse fluctuations written in Eq. (28) are

$$\begin{aligned}V_{\rm NL}(p+1,p)=&-\frac{2J_\perp}{N}\sum_{1,2,3,4,\mathbf{G}}\delta_{\mathbf{G}}l_1l_2l_3l_4e^{i\mathbf{G}\cdot\tau_1(p)}\\&\times[I^{(1)}_{1234}\alpha^+_p(1)\alpha^+_{p+1}(2)\beta^+_{p+1}(3)\beta^+_{p+1}(4)+I^{(2)}_{1234}\alpha^+_{p+1}(2)\beta^+_{p+1}(3)\beta^+_{p+1}(4)\beta_{p+1}(-1)\\&+I^{(3)}_{1234}\alpha^+_p(1)\beta^+_{p+1}(3)\beta^+_{p+1}(4)\beta_{p+1}(-2)+I^{(4)}_{1234}\beta^+_{p+1}(3)\beta^+_{p+1}(4)\beta_{p+1}(-2)\beta_p(-1)\\&+2I^{(5)}_{1234}\alpha^+_p(1)\alpha^+_{p+1}(2)\beta^+_{p+1}(3)\alpha_{p+1}(-4)+2I^{(6)}_{1234}\alpha^+_{p+1}(2)\beta^+_{p+1}(3)\beta_p(-1)\alpha_{p+1}(-4)\\&+2\tilde I^{(6)}_{1234}\alpha^+_p(1)\beta^+_{p+1}(4)\beta_{p+1}(-2)\alpha_{p+1}(-3)+2\tilde I^{(5)}_{1234}\beta^+_{p+1}(4)\beta_p(-1)\beta_{p+1}(-2)\alpha_{p+1}(-3)\\&+\tilde I^{(4)}_{1234}\alpha^+_p(1)\alpha^+_{p+1}(2)\alpha_{p+1}(-3)\alpha_{p+1}(-4)+\tilde I^{(3)}_{1234}\beta_p(-1)\alpha^+_{p+1}(2)\alpha_{p+1}(-3)\alpha_{p+1}(-4)\\&+\tilde I^{(2)}_{1234}\alpha^+_p(1)\beta_{p+1}(-2)\alpha_{p+1}(-3)\alpha_{p+1}(-4)+\tilde I^{(1)}_{1234}\beta_p(-1)\beta_{p+1}(-2)\alpha_{p+1}(-3)\alpha_{p+1}(-4)],\end{aligned} \tag{75}$$

$$\begin{aligned}V_{\rm NL}(p,p+1)=&-\frac{2J_\perp}{N}\sum_{1,2,3,4,\mathbf{G}}\delta_{\mathbf{G}}l_1l_2l_3l_4e^{i\mathbf{G}\cdot\tau_1(p)}\\&\times[I^{(7)}_{1234}\alpha^+_{p+1}(1)\alpha^+_p(2)\beta^+_p(3)\beta^+_p(4)+I^{(8)}_{1234}\alpha^+_p(2)\beta^+_p(3)\beta^+_p(4)\beta_{p+1}(-1)\\&+I^{(9)}_{1234}\alpha^+_{p+1}(1)\beta^+_p(3)\beta^+_p(4)\beta_p(-2)+I^{(10)}_{1234}\beta^+_p(3)\beta^+_p(4)\beta_{p+1}(-1)\beta_p(-2)\\&+2I^{(11)}_{1234}\alpha^+_{p+1}(1)\alpha^+_p(2)\beta^+_p(3)\alpha_p(-4)+2I^{(12)}_{1234}\alpha^+_p(2)\beta^+_p(3)\beta_{p+1}(-1)\alpha_p(-4)\\&+2\tilde I^{(12)}_{1234}\alpha^+_{p+1}(1)\beta^+_p(4)\beta_p(-2)\alpha_p(-3)+2\tilde I^{(11)}_{1234}\beta^+_p(4)\beta_{p+1}(-1)\beta_p(-2)\alpha_p(-3)\\&+\tilde I^{(10)}_{1234}\alpha^+_{p+1}(1)\alpha^+_p(2)\alpha_p(-3)\alpha_p(-4)+\tilde I^{(9)}_{1234}\beta_{p+1}(-1)\alpha^+_p(2)\alpha_p(-3)\alpha_p(-4)\\&+\tilde I^{(8)}_{1234}\alpha^+_{p+1}(1)\beta_p(-2)\alpha_p(-3)\alpha_p(-4)+\tilde I^{(7)}_{1234}\beta_{p+1}(-1)\beta_p(-2)\alpha_p(-3)\alpha_p(-4)],\end{aligned} \tag{76}$$

where

$$I^{(1)}_{1234}(\sigma_p\sigma_{p+1})=(1-x_1\gamma_{\mathbf{G}})(x_3x_4-x_2)c_{2+3+4}-\sigma_p\sigma_{p+1}(1+x_1\gamma_{\mathbf{G}})(x_3x_4+x_2)s_{2+3+4}, \tag{77}$$

$$I^{(3)}_{1234}(\sigma_p\sigma_{p+1})=(1-x_1\gamma_{\mathbf{G}})(1-x_2x_3x_4)c_{2+3+4}+\sigma_p\sigma_{p+1}(1+x_1\gamma_{\mathbf{G}})(1+x_2x_3x_4)s_{2+3+4}, \tag{78}$$

$$I^{(5)}_{1234}(\sigma_p\sigma_{p+1})=(1-x_1\gamma_{\mathbf{G}})(x_2x_4-x_3)c_{2+3+4}+\sigma_p\sigma_{p+1}(1+x_1\gamma_{\mathbf{G}})(x_2x_4+x_3)s_{2+3+4}. \tag{79}$$

The other coefficients are obtained from the relations obtained in Appendix D of Ref. 34:

$$I^{(2n)}_{1234}(\sigma)=\gamma_{\mathbf{G}}I^{(2n-1)}_{1234}(-\sigma), \tag{80}$$

$$\tilde I^{(n)}_{1234}(\sigma)=\gamma_{\mathbf{G}}I^{(n)}_{1234}(\sigma), \tag{81}$$

$$I^{(n+6)}_{1234}(\sigma)=e^{i[\tau_1(p+1)-\tau_1(p)]}I^{(n)}_{1234}(\sigma). \tag{82}$$

Before starting the calculations we make some preliminary remarks. First of all, we are interested only in terms of order j^4. So we only consider contributions which involve four powers of the interplane interactions, each of which could, in principle, be either the quadratic ones of Eq. (35) or the quartic ones of Eqs. (71) and (75). However, two will involve the coupling between planes 1 and 2 and two will involve the couping between planes 2 and 3. (We only need to consider three planes because four interplane perturbations cannot span four planes at order j^4.) From now on we therefore write $\sigma=\sigma_1\sigma_2$ and $\sigma'=\sigma_2\sigma_3$ and set $\sigma_1=1$. In other words, for plane 1, $\tau_1=0$, for plane 2,

$$\tau_1(2)=[(\sigma+1)\hat i+(1-\sigma)\hat j](a/4)\equiv\tau' \tag{83}$$

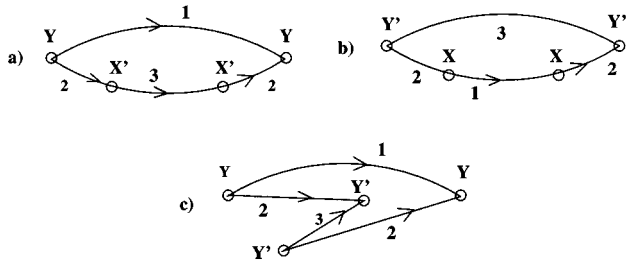

FIG. 3. The topologies of diagrams for the ground-state energy at relative order j^4S^{-1}. Here X and Y denote X_σ and Y_σ, respectively, and X' and Y' denote $X_{\sigma'}$ and $Y_{\sigma'}$, respectively. In diagrams a and b the ordering (to the right is forward going) of vertices is unique. In diagram c there are four ways to order the two Y' vertices with respect to the Y vertices. The labels indicate in which plane the propagation occurs, but all possible choices of polarization labels (α) must be included.

and for plane 3

$$\tau_1(3)=(1-\sigma\sigma')[\hat{i}+\hat{j}](a/4)\equiv\tau'' \tag{84}$$

are locations of up spins in these planes (see Fig. 2). Secondly, we have considered terms quadratic in the normal modes which result from normally ordering operators when we transformed to normal modes. As will become apparent, such terms do not contribute at the leading nonzero order in $1/S$. Thirdly, since we are studying the structure as influenced by quantum corrections, we will only analyze terms which are proportional to $\sigma\sigma'$. (By symmetry there can be no terms proportional to σ or to σ'.) In this connection we should note that $X_\sigma(\mathbf{q})Y_\sigma(\mathbf{q})$ is independent of σ. As a consequence, when we consider perturbative contributions involving two $V(i,j)$'s, we only keep diagrams having two X_σ's or two Y_σ's.

Now we carry out the calculations indicated above. We first consider the perturbative contribution to the energy of order j^4 at leading order in $1/S$. Such terms are represented by the diagrams[35] shown in Fig. 3, where we label the propagators according to the layer they are in.

In principle, we should also give each propagator an index, such as α or β for excitations in the first layer. However, in evaluating diagrams we will count the number of ways of assigning such labels. For instance, we find the sum of the contributions from Fig. 3 to be

$$\delta E=\frac{J_\perp^4 S}{\tilde{J}^3}\sum_{\mathbf{q}}\left[\frac{Y_\sigma(\mathbf{q})^2X_{\sigma'}(\mathbf{q})^2+X_\sigma(\mathbf{q})^2Y_{\sigma'}(\mathbf{q})^2}{(-2\epsilon_{\mathbf{q}})^3}+4\frac{Y_\sigma(\mathbf{q})^2Y_{\sigma'}(\mathbf{q})^2}{(-2\epsilon_{\mathbf{q}})^2(-4\epsilon_{\mathbf{q}})}\right]_{\sigma\sigma'}, \tag{85}$$

where $[\,]_{\sigma\sigma'}$ indicates the contribution of order $\sigma\sigma'$ that we want. Here the subscript on X and Y gives the value of $\sigma_p\sigma_{p+1}$. The prefactor to the sum in Eq. (85) includes a factor $(4J_\perp S)^4$ for the four interlayer interactions, $(8\tilde{J}S)^{-3}$ to scale the three energy denominators, and a factor of 2 corresponding to interchanging the roles of α and β. In Eq. (85) the factor 4 comes from the four different orderings of vertices possible for diagram (c) of Fig. 3. In particular, note the crucial σ-dependent parts of X^2 and Y^2:

$$[X_\sigma(\mathbf{q})^2]_\sigma=-[Y_\sigma(\mathbf{q})^2]_\sigma=2\sigma c_{\mathbf{q}}s_{\mathbf{q}}. \tag{86}$$

Using this result one sees that the contribution to the energy written in Eq. (85) vanishes. This result was expected, of course, because the work of Sec. III indicated that there was zero contribution to δE at order $SJ_\perp^4/J^3$.

At order S^0 (i.e., relative order S^{-2}) we have contributions such as those represented in Fig. 4, which involve a quartic intraplane interaction (in plane 2) and four quadratic interplane interactions or four interplane interactions, one of which is quartic. We label the wave vectors of the upper loop $\mathbf{k}$ and the lower loop $\mathbf{q}$. Then for the $\sigma\sigma'$-dependent terms from each diagram one see that in the sum over $\mathbf{q}$ the summand includes the factor $c_{\mathbf{q}}s_{\mathbf{q}}$ which is odd under interchange of q_x and q_y. Since the rest of the summand is an even under interchange of q_x and q_y, this sum over $\mathbf{q}$ vanishes. So, in this order we still get a vanishing contribution to the energy proportional to $\sigma\sigma'$. Note that the diagrams of

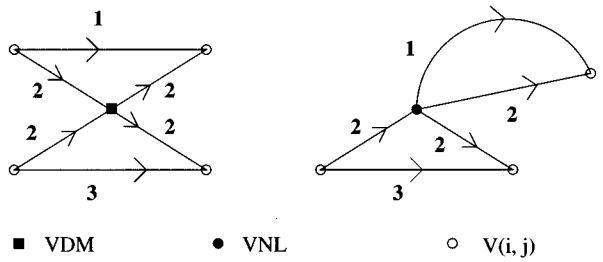

FIG. 4. As in Fig. 3, the topologies of diagrams at order 1. The quadratic vertices can be either X or Y, but to get a contribution proportional to $\sigma\sigma'$ two quadratic vertices in the same loop must either both be X or both be Y. Here VDM denotes $H_p^{(4)}$ and VNL denotes V_{NL}.

Figs. 3 and 4 give zero contributions to the energy even in the presence of the spin-wave renormalizations, $J\to\tilde{J}$ and $S\to\tilde{S}$.

Finally, we are led to consider the contribution to the energy proportional to $J_\perp^4\sigma\sigma'$ which is of order $1/S$. As we shall see, we obtain a nonzero result at this order in $1/S$. Accordingly, to get results at order j^4 which are correct to leading order in $1/S$ we henceforth set $\tilde{J}=J$ and $\tilde{S}=S$. At this order in $1/S$ there are six types of perturbative contributions, T_i for $i=1,6$, which are represented schematically in Fig. 5.

We consider the first type of term shown in Fig. 5. We show that these contributions involving two V_{zz}'s vanish. To see this consider the allowed ordering of vertices of this type. Note that the two quartic interplane interactions must be connected by three lines, all of which must go in the same direction. (For this analysis we use a diagrammatic formulation[35] in which only forward-going lines are allowed at zero temperature.) To obtain an allowed ordering we have only the diagrams (in which only forward-going lines occur) shown in Fig. 6. Note that in all cases, we need the square of an interplane matrix element, $H^{(1)}(1,2,3,4)$ or $H^{(2)}(1,2,3,4)$, which is given in Eqs. (72)–(74). There we see that the σ-dependent part of matrix element is proportional to $x_2^2-x_1^2$. Since the rest of the integrand is even under interchange of $\mathbf{k}_1$ and $\mathbf{k}_2$, such a factor vanishes when summed over $\mathbf{k}_1$ and $\mathbf{k}_2$. Thus $T_1=0$.

We now consider terms of type No. 2 of Fig. 5. The two possible topologies of diagrams of interest are those shown in Fig. 7. In the first two of these, the insertions of two

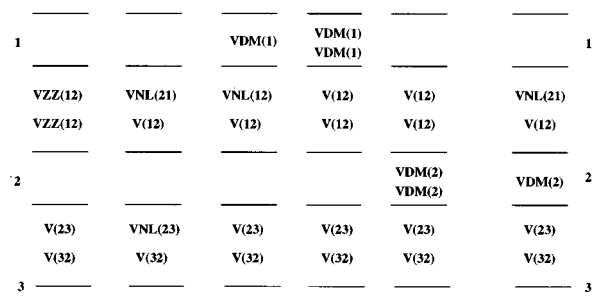

FIG. 5. The six types of perturbation terms, T_i, at order $1/S$. Here VZZ denotes V_{zz}, VNL denotes V_{NL}, and VDM(p) denotes $H_p^{(4)}$.

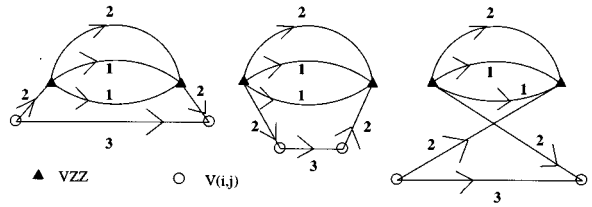

FIG. 6. Various types of contributions to T_1 of Fig. 5. For the right-most diagram there are four ways to order the vertices maintaining the directions assigned to each of the lines. For the left-most diagram the quartic vertices involve $H^{(2)}(1,2,3,4)$ and for the others the quartic vertices involve $H^{(1)}(1,2,3,4)$, where $\mathbf{q}_1$ and $\mathbf{q}_2$ are the wave vectors of the propagators for layer 1.

quadratic perturbations occur in the same line. Otherwise the insertions occur in different lines. Note that the quartic interlayer perturbations have no terms involving either $\alpha_p^+ \alpha_p^+$ or $\beta_p \beta_p$. What this means is that it is impossible to have a diagram with two lines of the same type (α or β) connecting the two quartic vertices in Fig. 7. This consideration indicates that the left-hand case of Fig. 7 cannot actually occur. Also, in the right-hand case the two lines with no insertion must be one of each type. Now we consider completing the quartic vertices with the other lines which do carry insertions.[36] For instance, the ''1'' vertex (i.e., the one with a ''1'' line) is completed by two additional lines. One of these is either a β_2 ($\beta_2 \equiv \delta$) outgoing line or an α_2 ($\alpha_2 \equiv \gamma$) incoming line. The other is either an α_1 ($\alpha_1 \equiv \alpha$) outgoing line or a β_1 ($\beta_1 \equiv \beta$) incoming line. The ''3'' vertex (i.e., the one which a ''3'' line) is also completed by two additional lines, one of which is either an α_2 ($\alpha_2 \equiv \gamma$) incoming line or a β_2 ($\beta_2 \equiv \delta$) outgoing line. The other is either an α_3 ($\alpha_3 \equiv \rho$) outgoing line or a β_3 ($\beta_3 \equiv \eta$) incoming line. Bearing in mind that when time ordered, these diagrams must not have any backward-going (i.e., leftward) lines, we have the possible diagrams shown in Fig. 8.

Each of the diagrams in Fig. 8 gives rise to one or two time-ordered diagrams.[35] For instance, diagram 1 of Fig. 8 can have the quadratic vertices in either of two time sequences. In diagram 2 of Fig. 8 only one time ordering is possible. (The quadratic perturbation of the second line down from the top must occur to the right of the quartic vertices in order for the two parts of this line to be forward going.)

For the diagrams in Fig. 8 we get the respective contributions to the energy

$$T_{2,i} = -\frac{1}{4}\frac{J_\perp^4}{J^3 S}\frac{1}{N^2}\sum_{1,2,3,4} \delta_{\mathbf{G}} l_1^2 l_2^2 l_3^2 l_4^2 [t_i^{(2)}]_{\sigma\sigma'}, \qquad (87)$$

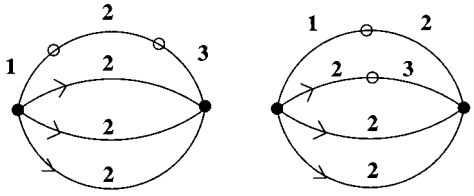

FIG. 7. The two topologies for T_2 of Fig. 5. The diagram on the left does not exist, as is discussed in the text. The legend for the interactions is shown in Fig. 4.

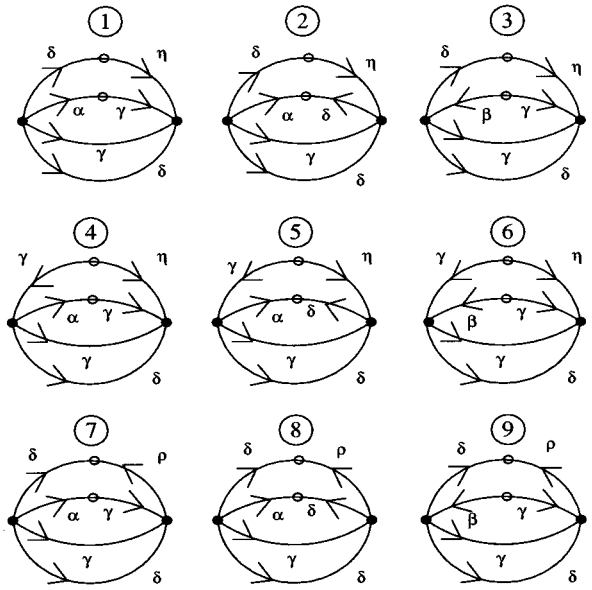

FIG. 8. The nine vertices of type T_{2i}. In all cases the vertex $V_{\mathrm{NL}}(21)$ always comes to the left (before) the vertex $V_{\mathrm{NL}}(23)$. The internal perturbations should be distributed over all time orderings such that all lines are forward going (i.e., have their arrows pointing to the right). There is a one-to-one correspondence between these diagrams and those in which $V_{\mathrm{NL}}(21)$ comes to the right of $V_{\mathrm{NL}}(23)$. Here and in succeeding figures $\alpha \equiv \alpha_1$, $\beta \equiv \beta_1$, $\gamma \equiv \alpha_2$, $\delta \equiv \beta_2$, $\rho \equiv \alpha_3$, and $\eta \equiv \beta_3$. The legend for the interactions is shown in Fig. 4. In all figures we label lines with wave vectors $\mathbf{q}_1 \equiv 1$, $\mathbf{q}_2 \equiv 2$, $\mathbf{q}_3 \equiv 3$, $\mathbf{q}_4 \equiv 4$, starting from the top.

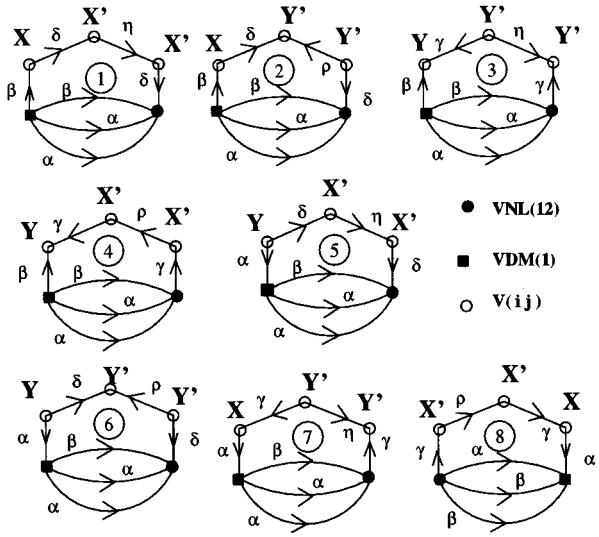

FIG. 9. The allowed labelings (1–7) of diagrams of type T_3 with V_{DM} first. Diagrams with V_{NL} first are obtained from those with V_{DM} first by (a) reversing the direction of the time arrows on each line and (b) interchanging labels: ($\alpha \leftrightarrow \beta$, $\gamma \leftrightarrow \delta$, $\eta \leftrightarrow \rho$). To illustrate, we show the diagram, (8), which is obtained by this procedure from diagram 1. The contribution of each such transformed diagram is the same as that of its antecedent.

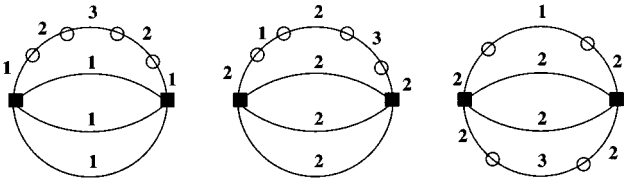

FIG. 10. Left: The topology of diagrams of the type T_4. Center: The topology of similar diagrams of type T_5. Right: topology of diagrams of type T_5 with insertions on two different legs. (Contributions from the former are denoted T_{5a} and from the latter T_{5b}.) The legend for interactions is the same as in Fig. 3.

where the prefactor comes from (a) 2 for the two orderings of the quartic vertices: "1" before "3" and "3" before "1" (In Fig. 8 we only show "1" to the left of "3"), (b) $(-2J_\perp/N)^2$ from the nonlinear interactions, (c) $(4J_\perp S)^2$ from the linear interactions, (d) $(8JS)^3$ to scale the energy denominators, and (e) an overall minus sign. We have the results:

$$t_1^{(2)}=e^{i\mathbf{G}\cdot\tau'(\sigma)}\frac{2}{\Delta^3}X_{\sigma'}(1)X_\sigma(2)I^{(1)}_{2341}(\sigma)\tilde{I}^{(7)}_{1432}(\sigma')4,$$

$$t_2^{(2)}=e^{i\mathbf{G}\cdot\tau'(\sigma)}\frac{1}{2\epsilon_2\Delta^2}X_{\sigma'}(1)Y_\sigma(2)I^{(1)}_{2341}(\sigma)2\tilde{I}^{(11)}_{1432}(\sigma')2,$$

$$t_3^{(2)}=e^{i\mathbf{G}\cdot\tau'(\sigma)}\frac{1}{2\epsilon_2\Delta^2}X_{\sigma'}(1)Y_\sigma(2)I^{(2)}_{2341}(\sigma)\tilde{I}^{(7)}_{1432}(\sigma')4,$$

$$t_4^{(2)}=e^{i\mathbf{G}\cdot\tau'(\sigma)}\frac{1}{2\epsilon_1\Delta^2}Y_{\sigma'}(1)X_\sigma(2)2I^{(5)}_{2341}(\sigma)\tilde{I}^{(7)}_{1432}(\sigma')2,$$

$$t_5^{(2)}=e^{i\mathbf{G}\cdot\tau'(\sigma)}\frac{1}{4\epsilon_1\epsilon_2\Delta}Y_{\sigma'}(1)Y_\sigma(2)2I^{(5)}_{2341}(\sigma)2\tilde{I}^{(11)}_{1432}(\sigma')1,$$

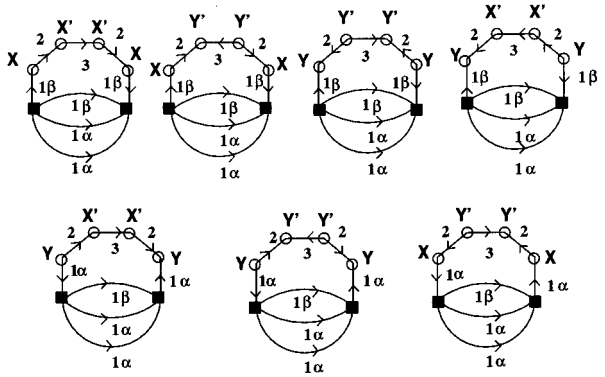

FIG. 11. Seven ways to assign directions to the topology of type T_4. The diagram are numbered 1 through 7 in reading order. Here $X\equiv X_\sigma$, $X'\equiv X_{\sigma'}$, etc. The legend for interactions is the same as in Fig. 3.

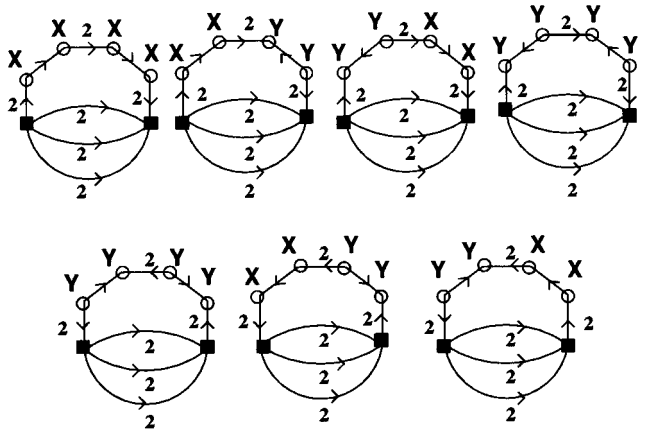

FIG. 12. Various ways to assign directions to the topology of type T_{5a}. In each diagram one of the unlabeled lines is a "1" and the other is a "3." The contribution from each of these two choices of labelings is the same. The legend for interactions is the same as in Fig. 3.

$$t_6^{(2)}=e^{i\mathbf{G}\cdot\tau'(\sigma)}\frac{1}{4\epsilon_1\epsilon_2\Delta}Y_{\sigma'}(1)Y_\sigma(2)2I^{(6)}_{2341}(\sigma)\tilde{I}^{(7)}_{1432}(\sigma')2,$$

$$t_7^{(2)}=e^{i\mathbf{G}\cdot\tau'(\sigma)}\frac{1}{2\epsilon_1\Delta^2}Y_{\sigma'}(1)X_\sigma(2)I^{(1)}_{2341}(\sigma)\tilde{I}^{(8)}_{1432}(\sigma')4,$$

$$t_8^{(2)}=e^{i\mathbf{G}\cdot\tau'(\sigma)}\frac{1}{4\epsilon_1\epsilon_2\Delta}Y_{\sigma'}(1)Y_\sigma(2)I^{(1)}_{2341}(\sigma)2\tilde{I}^{(12)}_{1432}(\sigma')2,$$

$$t_9^{(2)}=e^{i\mathbf{G}\cdot\tau'(\sigma)}\frac{1}{4\epsilon_1\epsilon_2\Delta}Y_{\sigma'}(1)Y_\sigma(2)I^{(2)}_{2341}(\sigma)\tilde{I}^{(8)}_{1432}(\sigma')4, \tag{88}$$

where $\Delta=\epsilon_1+\epsilon_2+\epsilon_3+\epsilon_4$ and the final factor is the multiplicity of the graph (i.e., the number of ways the contractions can be made) and the first factor is the appropriate sum of the energy denominators over all time orderings. The above results are simplified in Appendix E of Ref. 34 where the final result is

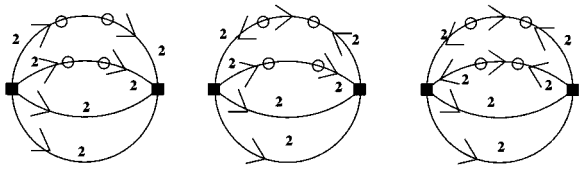

FIG. 13. Topology of diagrams that contribute to $A_{++}(m,n)$ of Eq. (109) (left panel), to $A_{-+}(l,m)$ of Eq. (113) (right panel), where m and n are momentum labels of lines (starting with 1 for the top line and going to 4 for the bottom line). Any line without an arrow can be assigned either direction and can be made forward going by suitable time ordering of the perturbations. In each diagram one of the unlabeled lines is a "1" and the other is a "3." The contribution from each of these two choices of labelings is the same.

$$T_2=\frac{2J_\perp^4\sigma\sigma'}{J^3S}\frac{1}{N^2}\sum_{1,2,3,4}\delta_{\mathbf{G}}l_1^2l_2^2l_3^2l_4^2c_1s_1c_2s_2\left\{\left(\frac{4}{\Delta^3}-\frac{1}{\Delta^2\epsilon_1}-\frac{1}{\Delta^2\epsilon_2}+\frac{1}{\Delta\epsilon_1\epsilon_2}\right)(x_1x_4-\gamma_{\mathbf{G}}x_2x_3)^2\right.$$
$$\left.-\left(\frac{1}{\Delta\epsilon_1\epsilon_2}-\frac{1}{\Delta^2\epsilon_1}-\frac{1}{\Delta^2\epsilon_2}\right)(x_4-x_1x_2x_3\gamma_{\mathbf{G}})^2\right\}. \tag{89}$$

We now consider the T_3 terms shown in Fig. 5. We see that the V_{23}'s must come together to form a renormalized 2-2 line. Also recall that $[X'_\sigma Y'_\sigma]_\sigma=0$. So the only allowed diagrams are those shown in Fig. 9. We write

$$T_3=\frac{J_\perp^4}{4J^3S}\frac{1}{N^2}\sum_{1,2,3,4}\delta_{\mathbf{G}}l_1^2l_2^2l_3^2l_4^2\sum_{i=1,9}t_i^{(3)}. \tag{90}$$

Here the prefactor reflects (a) a factor of 2 because we could consider $V_{\rm NL}(3,2)$ instead of $V_{\rm NL}(1,2)$, (b) a factor of 2 as to which vertex comes earlier in time, (c) $-2J/N$ from the D-M perturbation, (c) $(4J_\perp S)^3$ for the linear interactions, (d) $-2J_\perp/N$ for the nonlinear interaction, and (e) $(8JS)^4$ in the denominator for the energies. Note that $t_i^{(3)}$ includes both matrix elements and the energy denominators, summed over all allowed time orderings.

We find that

$$t_1^{(3)}=-2\sigma' c_1s_1[X_\sigma(1)\tilde I^{(7)}_{1234}(\sigma)]_\sigma\Phi^{(7)}_{3412}\left(\frac{1}{\Delta^4}\right)(4), \tag{91}$$

$$t_2^{(3)}=2\sigma' c_1s_1[X_\sigma(1)\tilde I^{(7)}_{1234}(\sigma)]_\sigma\Phi^{(7)}_{3412}\left(\frac{1}{\Delta^3(2\epsilon_1)}+\frac{1}{\Delta^2(2\epsilon_1)^2}+\frac{1}{\Delta(2\epsilon_1)^3}\right)(4), \tag{92}$$

$$t_3^{(3)}=2\sigma' c_1s_1[Y_\sigma(1)\tilde I^{(8)}_{1234}(\sigma)]_\sigma\Phi^{(7)}_{3412}\left(\frac{1}{4\epsilon_1^3\Delta}+\frac{1}{4\epsilon_1^2\Delta^2}\right)(4), \tag{93}$$

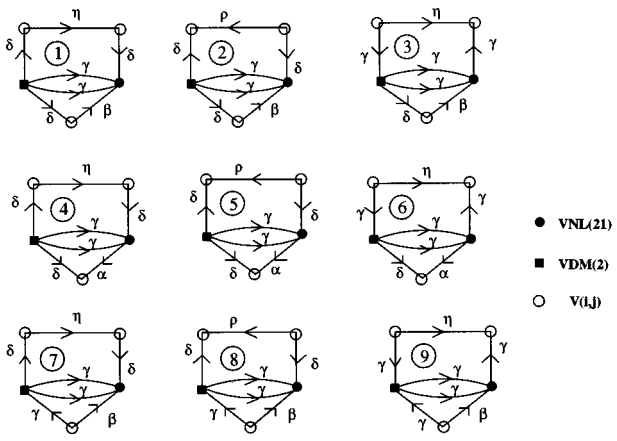

FIG. 14. Various ways, ($i=1,9$), to assign directions to the topology of type T_{6a}. Further ways are shown in Fig. 15.

$$t_4^{(3)}=-2\sigma' c_1s_1[Y_\sigma(1)\tilde I^{(8)}_{1234}(\sigma)]_\sigma\Phi^{(7)}_{3412}\left(\frac{1}{\Delta(2\epsilon_1)^3}\right)(4), \tag{94}$$

$$t_5^{(3)}=-2\sigma' c_1s_1[Y_\sigma(1)\tilde I^{(7)}_{1234}(\sigma)]_\sigma[2\Phi^{(3)}_{3412}]\left(\frac{1}{\Delta^3(2\epsilon_1)}+\frac{1}{\Delta^2(2\epsilon_1)^2}+\frac{1}{\Delta(2\epsilon_1)^3}\right)(2), \tag{95}$$

$$t_6^{(3)}=2\sigma' c_1s_1[Y_\sigma(1)\tilde I^{(7)}_{1234}(\sigma)]_\sigma[2\Phi^{(3)}_{3412}]\left(\frac{1}{4\epsilon_1^3\Delta}+\frac{1}{4\epsilon_1^2\Delta^2}\right)\times(2), \tag{96}$$

$$t_7^{(3)}=2\sigma' c_1s_1[X_\sigma(1)\tilde I^{(8)}_{1234}(\sigma)]_\sigma[2\Phi^{(3)}_{3412}]\left(\frac{1}{\Delta(2\epsilon_1)^3}\right)(2). \tag{97}$$

In writing these results we used Eq. (86). We also used results for the sums of energy denominators over allowed time ordering of vertices from Appendix F of Ref. 34. These results are simplified in Appendix F (Ref. 34) into the form

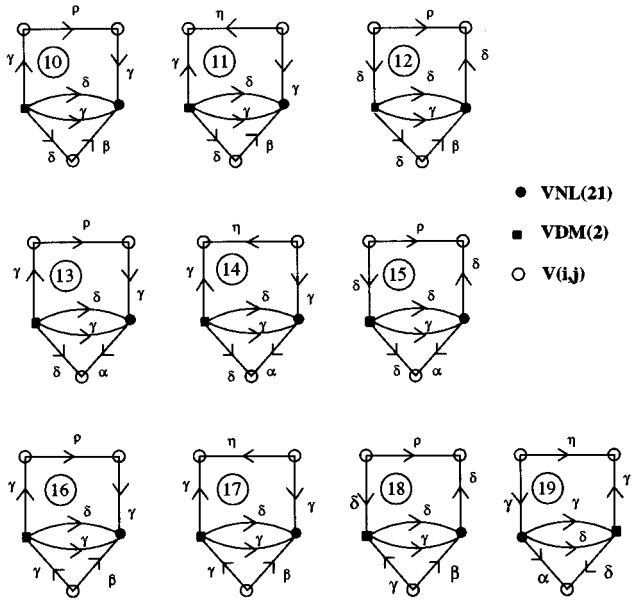

FIG. 15. Further ways, ($i=10,18$), to assign directions to the topology of type T_{6a}. The last diagram (19) is one with $V_{\rm NL}$ to the left of $V_{\rm DM}$ and is obtained from diagram 18 by replacing β by α^+, etc., as explained in the caption to Fig. 9. Its contribution is the same as diagram 18.

$$T_3=\frac{J_\perp^4\sigma\sigma'}{J^3S}\frac{1}{N^2}\sum_{1,2,3,4}\delta_{\mathbf{G}}l_1^2l_2^2l_3^2l_4^2c_1^2s_1^2\left\{\Phi^{(7)}_{3412}(\gamma_{\mathbf{G}}x_3x_4-x_1x_2)\left(\frac{4}{\Delta^4}-\frac{2}{\epsilon_1\Delta^3}\right)+(x_2-\gamma_{\mathbf{G}}x_1x_3x_4)\Phi^{(3)}_{3412}\left(\frac{2}{\epsilon_1\Delta^3}\right)\right\}. \quad (98)$$

In the terms of the type T_4 of Fig. 5, it is easily seen that the $V(2,3)$'s must be connected to give a renormalized propagator for momentum 2. The only way to now contract the 2 lines is to use this renormalized propagator to connect the two $V(1,2)$'s. We therefore have the topology shown in the left panel of Fig. 10.

Since we know that we must be able to make a time ordered diagram with no backward lines, the three lines with no insertions must all be in the same direction. Given this, the possible directions of the lines for T_4 terms are as shown in Fig. 11. Also we must not use $X_\sigma(1)Y_\sigma(1)$ since that quantity does not depend on σ. Similar reasoning applies to $X_{\sigma'}(1)Y_{\sigma'}(1)$.

We write

$$T_4=-\frac{J_\perp^4}{16J^3SN^2}\sum_{1,2,3,4,\mathbf{G}}\delta_{\mathbf{G}}l_1^2l_2^2l_3^2l_4^2t_i^{(4)}, \quad (99)$$

where we took factors (a) 2 for interchanging the roles of "1" and "3," (b) $(-2J/N)^2$ for the two Dyson-Maleev vertices, (c) $(4J_\perp S)^4$ for the linear interplane interactions, and (e) $(-8JS)^5$ to scale the energy denominators. Then, from Appendix G of Ref. 34 we have that

$$\sum_{i=1,4}t_i^{(4)}=4\sigma\sigma'c_1^2s_1^2(4)[2\Phi^{(7)}_{3412}\Phi^{(8)}_{1234}+2\Phi^{(7)}_{1234}\Phi^{(8)}_{3412}]\left[\frac{16\epsilon_1^4-8\epsilon_1^3\Delta-\Delta^4}{16\epsilon_1^4\Delta^5}\right], \quad (100)$$

where we took account of the fact that the insertions could take place in any of the four forward-going lines. In Appendix G (Ref. 34) we obtain

$$\sum_{i=5,7}t_i^{(4)}=-4\sigma\sigma'c_1^2s_1^2(2)[(2\Phi^{(3)}_{3412})(2\Phi^{(2)}_{1234})+(2\Phi^{(6)}_{1234})(2\Phi^{(5)}_{3412})]\left(\frac{4\epsilon_1^3+2\epsilon_1\Delta+\Delta^2}{16\epsilon_1^4\Delta^3}\right). \quad (101)$$

Therefore we have

$$T_4=-\frac{2J_\perp^4\sigma\sigma'}{J^3SN^2}\sum_{1,2,3,4,\mathbf{G}}\delta_{\mathbf{G}}l_1^2l_2^2l_3^2l_4^2c_1^2s_1^2\left\{(\Phi^{(7)}_{3412}\Phi^{(8)}_{1234})\frac{16\epsilon_1^4-8\epsilon_1^3\Delta-\Delta^4}{8\epsilon_1^4\Delta^5}-(\Phi^{(3)}_{3412}\Phi^{(2)}_{1234})\frac{4\epsilon_1^2+2\epsilon_1\Delta+\Delta^2}{8\epsilon_1^4\Delta^3}\right\}. \quad (102)$$

Of the terms of type T_5 there are two subtypes: in the first subtype (T_{5a}, shown in the center panel of Fig. 10) we put all the insertions in the same leg. The resulting diagrams (shown in Fig. 12) will have sums over energy denominators which can be related to those of type T_4 (shown in Fig. 11). Thus we write

$$T_{5a}=-\frac{J_\perp^4}{16J^3SN^2}\sum_{1,2,3,4\mathbf{G}}\delta(1+2+3+4-\mathbf{G})l_1^2l_2^2l_3^2l_4^2t_i^{(5a)}. \quad (103)$$

Here we again have the factor of 2 in the prefactor because of the degeneracy between the labels "1" and "3." The first four diagrams correspond to contractions of a $\Phi^{(7)}$ and a $\Phi^{(8)}$, whereas the last three correspond to contracting either a $\Phi^{(3)}$ and a $\Phi^{(2)}$ or a $\Phi^{(6)}$ and a $\Phi^{(5)}$. However, the S factors for the energy denominators is different here than for T_4. We have

$$S_1^{(5a)}=S_1^{(4)},\quad S_2^{(5a)}=S_3^{(5a)}=S_2^{(4)},\quad S_4^{(5a)}=S_3^{(4)},\quad S_5^{(5a)}=S_4^{(4)},\quad S_6^{(5a)}=S_7^{(5a)}=S_7^{(4)}. \quad (104)$$

Thus, using Eq. (86), we have

$$\sum_{i=1,4}t_i^{(5a)}=4\sigma\sigma'c(1)^2s(1)^2[2\Phi^{(7)}_{3412}\Phi^{(8)}_{1234}+2\Phi^{(7)}_{1234}\Phi^{(8)}_{3412}](4)[S_1^{(4)}-2S_2^{(4)}+S_3^{(4)}] \quad (105)$$

and

$$\sum_{i=5,7}t_i^{(5a)}=4\sigma\sigma'c(1)^2s(1)^2[(2\Phi^{(3)}_{3412})(2\Phi^{(2)}_{1234})+(2\Phi^{(6)}_{1234})(2\Phi^{(5)}_{3412})](2)[S_4^{(4)}-2S_7^{(4)}]. \quad (106)$$

So

$$T_{5a}=-\frac{4J_\perp^4\sigma\sigma'}{J^3SN^2}\sum_{1,2,3,4\mathbf{G}}\delta_{\mathbf{G}}l_1^2l_2^2l_3^2l_4^2c_1^2s_1^2\left[\Phi^{(7)}_{3412}\Phi^{(8)}_{1234}\frac{16\epsilon_1^4-16\epsilon_1^3\Delta-4\epsilon_1^2\Delta^2+\Delta^4}{16\epsilon_1^4\Delta^5}+\Phi^{(3)}_{3412}\Phi^{(2)}_{1234}\frac{\Delta+2\epsilon_1}{16\epsilon_1^4\Delta^2}\right]. \quad (107)$$

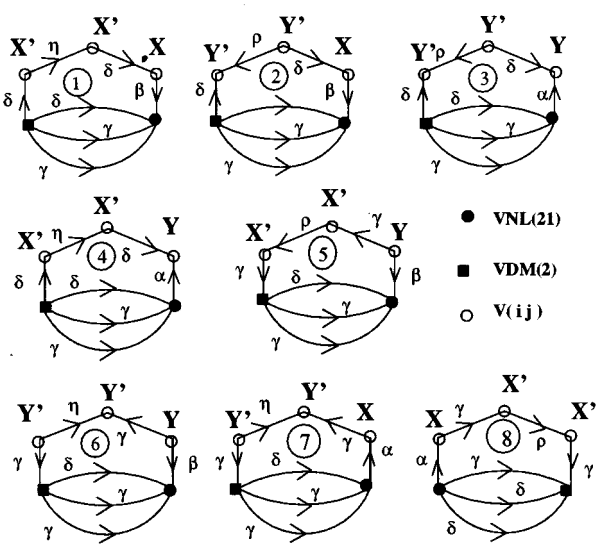

FIG. 16. The allowed labeling (1–7) of diagrams of the type T_{6b} with $V_{\rm DM}$ first. Diagrams with $V_{21}^{\rm NL}$ first (obtained by the transformation shown in Fig. 9) give the same contributions. For example, diagram 8 gives the same contribution as diagram 1.

The second, and new, type has insertions on two different legs. (This was not possible within type T_4.) The possible assignment of directions of lines is shown in Fig. 13. The corresponding evaluation of their energy denominators summed over all possible time orderings is now obtained by the same formalism as was used above for T_4.

Now we discuss in more detail how to put all this together for T_{5b}. (More details are given in Appendix H of Ref. 34.) Clearly the best way to think about these diagrams is to start with the entire family of diagrams generated by two Dyson-Maleev quartic interactions with at most two backward lines. Then we select two legs (including all the backward legs) for insertions. If all four lines are forward going we therefore have six choices for the two lines in which to make insertions. If we have only two forward lines in the bare diagram, then we must make insertions on both backward lines. We write

$$T_{5b}=-\frac{(-2J/N)^2}{(8JS)^5}(4J_\perp S)^4\sum_{1,2,3,4,\mathbf{G}}\delta_{\mathbf{G}}l_1^2l_2^2l_3^2l_4^2\sum_{i=1,3}t_i^{(5b)}, \tag{108}$$

where $t_i^{(5b)}$ comes from insertions in diagrams with $i-1$ backward lines. These three cases are shown in Fig. 13. We are only interested in the contributions proportional to $\sigma\sigma'$. Here the factors $-2J/N$ come from the Dyson-Maleev perturbation, the $8JS$ is for each energy denominator, and each interplane linear interaction carries a factor $4J_\perp S$.

Thus we have

$$t_1^{(5b)}=2\Phi_{3412}^{(7)}\Phi_{1234}^{(8)}(4)(\sigma\sigma')[A_{++}(1,2)+A_{++}(1,3)+A_{++}(1,4)+A_{++}(2,3)+A_{++}(2,4)+A_{++}(3,4)], \tag{109}$$

where A_{++} takes account of the possible arrow assignments in Fig. 13:

$$A_{++}(1,2)=\left[\frac{6}{\Delta^5}-\frac{3(\epsilon_1+\epsilon_2)}{2\Delta^4\epsilon_1\epsilon_2}-\frac{\epsilon_1^2+\epsilon_2^2}{4\Delta^3\epsilon_1^2\epsilon_2^2}+\frac{1}{2\epsilon_1\epsilon_2\Delta^3}+\frac{\epsilon_1+\epsilon_2}{8\epsilon_1^2\epsilon_2^2\Delta^2}+\frac{1}{16\epsilon_1^2\epsilon_2^2\Delta}\right]4c_1s_1c_2s_2. \tag{110}$$

Note that in Eq. (109) we included a factor of 2 for the degeneracy between labels "1" and "3" in the insertions. The factors $2cs$ come from the σ-dependent parts of X and Y. Recall that we have the restriction that in each leg either 2 X's or two Y's (but *not* XY) can appear to get the σ dependence. Likewise

$$t_2^{(5b)}=2[(2\Phi_{3412}^{(3)})(2\Phi_{1234}^{(2)})+(2\Phi_{1234}^{(6)})(2\Phi_{3412}^{(5)})]\times(2)(\sigma\sigma')[A_{-+}(1,2)+A_{-+}(1,3)+A_{-+}(1,4)], \tag{111}$$

where the insertion factor A_{-+} is given by

$$A_{-+}(1,2)=\left(\frac{2\epsilon_2+\Delta}{16\epsilon_1^2\epsilon_2^2\Delta^2}-\frac{1}{4\epsilon_1^2\Delta^3}\right)4c_1s_1c_2s_2. \tag{112}$$

Finally,

$$t_3^{(5b)}=2(4\Phi_{3412}^{(1)}\Phi_{1234}^{(1)}+4\Phi_{3412}^{(9)}\Phi_{1234}^{(9)}+(4\Phi_{3124}^{(4)})\times(4\Phi_{2431}^{(4)}))A_{--}(1,2)\sigma\sigma', \tag{113}$$

where

$$A_{--}(1,2)=\frac{1}{4\epsilon_1^2\epsilon_2^2\Delta}c_1s_1c_2s_2. \tag{114}$$

To summarize this result, we write $T_{5b}=T_{5bA}+T_{5bB}$, with

$$T_{5bA}=\frac{J_\perp^4\sigma\sigma'}{J^3SN^2}\sum_{1,2,3,4,\mathbf{G}}l_1^2l_2^2l_3^2l_4^2\delta_{\mathbf{G}}c_1s_1c_2s_2\left\{\Phi_{3412}^{(7)}\Phi_{1234}^{(8)}\left(-\frac{12}{\Delta^5}+\frac{3(\epsilon_1+\epsilon_2)}{\Delta^4\epsilon_1\epsilon_2}+\frac{\epsilon_1^2+\epsilon_2^2}{2\Delta^3\epsilon_1^2\epsilon_2^2}-\frac{1}{\epsilon_1\epsilon_2\Delta^3}-\frac{\epsilon_1+\epsilon_2}{4\epsilon_1^2\epsilon_2^2\Delta^2}-\frac{1}{8\epsilon_1^2\epsilon_2^2\Delta}\right)+\Phi_{3412}^{(3)}\Phi_{1234}^{(2)}\left(\frac{1}{\epsilon_1^2\Delta^3}-\frac{1}{2\epsilon_1^2\epsilon_2\Delta^2}-\frac{1}{4\epsilon_1^2\epsilon_2^2\Delta}\right)-\frac{1}{8\epsilon_1^2\epsilon_2^2\Delta}\Phi_{3412}^{(1)}\Phi_{1234}^{(1)}\right\} \tag{115}$$

and with a change of some momentum labels,

$$T_{5bB}=\frac{J_\perp^4\sigma\sigma'}{J^3SN^2}\sum_{1,2,3,4,\mathbf{G}} l_1^2l_2^2l_3^2l_4^2\delta_{\mathbf{G}}c_1s_1c_2s_2\Bigg\{\Phi^{(7)}_{2413}\Phi^{(8)}_{1324}\Bigg(-\frac{24}{\Delta^5}+\frac{(8\epsilon_1+4\epsilon_2)}{\Delta^4\epsilon_1\epsilon_2}+\frac{2}{\Delta^3\epsilon_2^2}-\frac{2}{\epsilon_1\epsilon_2\Delta^3}-\frac{1}{\epsilon_1\epsilon_2^2\Delta^2}-\frac{1}{4\epsilon_1^2\epsilon_2^2\Delta}\Bigg)$$
$$+\Phi^{(3)}_{2413}\Phi^{(2)}_{1324}\Bigg(\frac{2}{\epsilon_1^2\Delta^3}-\frac{1}{\epsilon_1^2\epsilon_2\Delta^2}-\frac{1}{2\epsilon_1^2\epsilon_2^2\Delta}\Bigg)-\frac{1}{4\epsilon_1^2\epsilon_2^2\Delta}\Phi^{(4)}_{3124}\Phi^{(4)}_{2431}\Bigg\}. \tag{116}$$

The diagrams of the type T_6 are again of two subtypes, T_{6a} in which the two insertions occur on different legs and T_{6b} in which all the insertions occur on the same leg. The former are shown in Fig. 14. Now we put this all together. (For more details of the evaluation of T_6 see Appendix I of Ref. 34.) For the diagrams of Fig. 14 we have the following contribution A to T_{6a}:

$$T_{6aA}=2(2)(-2J/N)(4J_\perp S)^3(-2J_\perp/N)(8JS)^{-4}\sigma'\sum_{1,2,3,4,\mathbf{G}} l_1^2l_2^2l_3^2l_4^2\delta_{\mathbf{G}}$$
$$\times 2c_1s_1b\Bigg(e^{i\mathbf{G}\cdot\tau'}\Bigg\{\Phi^{(7)}_{2314}\Bigg[\tilde I^{(1)}_{4123}(\sigma)X_\sigma(4)\Bigg(-\frac{3}{\Delta^3}+\frac{\Delta+4\epsilon_1}{\Delta^3(2\epsilon_1)^2}\Bigg)(4)$$
$$+\tilde I^{(2)}_{4123}(\sigma)Y_\sigma(4)\Bigg(-\frac{1}{\Delta^3(2\epsilon_4)}+\frac{1}{(2\epsilon_1)^2(2\epsilon_4)\Delta}+\frac{1}{(2\epsilon_1)(2\epsilon_4)\Delta^2}+\Bigg)(4)\Bigg]$$
$$+2\Phi^{(3)}_{2341}\tilde I^{(1)}_{4123}(\sigma)Y_\sigma(4)\Bigg(-\frac{1}{(2\epsilon_4)\Delta^3}+\frac{1}{(2\epsilon_1)^2(2\epsilon_4)\Delta}+\frac{1}{(2\epsilon_1)(2\epsilon_4)\Delta^2}+\Bigg)(2)$$
$$+2\Phi^{(3)}_{2314}\Bigg[\tilde I^{(3)}_{4123}X_\sigma(4)\frac{1}{(2\epsilon_1)^2\Delta^2}(2)+\tilde I^{(4)}_{4123}Y_\sigma(4)\frac{1}{(2\epsilon_1)^2(2\epsilon_4)\Delta}(2)\Bigg]+\Phi^{(1)}_{2314}\tilde I^{(3)}_{4123}Y_\sigma(4)\frac{1}{(2\epsilon_1)^2(2\epsilon_4)\Delta}(4)\Bigg\}\Bigg) \tag{117}$$

and for those of Fig. 15 we have the contribution B to T_{6a}:

$$T_{6aB}=2(2)(-2J/N)(4J_\perp S)^3(-2J_\perp/N)(8JS)^{-4}\sigma'\sum_{1,2,3,4,\mathbf{G}} l_1^2l_2^2l_3^2l_4^2\delta_{\mathbf{G}}$$
$$\times 2c_1s_1b\Bigg(e^{i\mathbf{G}\cdot\tau'}\Bigg\{\Phi^{(7)}_{1342}\Bigg[\tilde I^{(1)}_{4213}(\sigma)X_\sigma(4)\Bigg(\frac{3}{\Delta^4}+\frac{\Delta+4\epsilon_1}{\Delta^3(2\epsilon_1)^2}\Bigg)(8)$$
$$+\tilde I^{(2)}_{4213}(\sigma)Y_\sigma(4)\Bigg(\frac{1}{(2\epsilon_4)\Delta^3}+\frac{1}{(2\epsilon_1)^2(2\epsilon_4)\Delta}+\frac{1}{(2\epsilon_1)(2\epsilon_4)\Delta^2}\Bigg)(8)\Bigg]$$
$$+2\Phi^{(3)}_{1342}\tilde I^{(1)}_{4213}(\sigma)Y_\sigma(4)\Bigg(-\frac{1}{(2\epsilon_4)\Delta^3}+\frac{1}{(2\epsilon_1)^2(2\epsilon_4)\Delta}+\frac{1}{(2\epsilon_1)(2\epsilon_4)\Delta^2}\Bigg)(4)$$
$$+2\Phi^{(6)}_{1324}\Bigg[2\tilde I^{(5)}_{4231}X_\sigma(4)\frac{1}{(2\epsilon_1)^2\Delta^2}(2)+2\tilde I^{(6)}_{4231}Y_\sigma(4)\frac{1}{(2\epsilon_1)^2(2\epsilon_4)\Delta}(2)\Bigg]+4\Phi^{(4)}_{3142}2\tilde I^{(5)}_{4231}Y_\sigma(4)\frac{1}{(2\epsilon_1)^2(2\epsilon_4)\Delta}\Bigg\}\Bigg). \tag{118}$$

The factors here are 2 for the two orderings of $V_{\rm NL}$ and $V_{\rm DM}$, 2 for using VNL(2,3) rather than VNL(2,1), $(-2J/N)$ for $V_{\rm DM}$, $(-2J_\perp/N)$ for $V_{\rm NL}$, $(4J_\perp S)$ for each linear interplane interaction, and $(8JS)$ for each energy denominator. Also, the last factor in parenthesis for each diagram is the number of ways of contracting lines for that diagram, (4) for $\Phi^{(7)}$, for instance. Note that $V_{\rm DM}$ carries a factor $e^{i\mathbf{G}\cdot\tau'}$. Also note that the contraction factors are twice as large for (B) than for (A) because the latter has two equivalent choices for diagrams in which to put insertions. These are evaluated to be

$$T_{6aA}=\frac{J_\perp^4\sigma\sigma'}{J^3SN^2}\sum_{1,2,3,4,\mathbf{G}} l_1^2l_2^2l_3^2l_4^2\delta_{\mathbf{G}}c_1s_1c_2s_2\Bigg\{\Phi^{(7)}_{3412}(x_1x_2-\gamma_{\mathbf{G}}x_3x_4)\Bigg(-\frac{12}{\Delta^4}+\frac{4}{\epsilon_1\Delta^3}+\frac{2}{\epsilon_2\Delta^3}+\frac{1}{\epsilon_1^2\Delta^2}-\frac{1}{\epsilon_1\epsilon_2\Delta^2}-\frac{1}{2\epsilon_1^2\epsilon_2\Delta}\Bigg)$$
$$+\Phi^{(3)}_{3412}(x_3x_4x_1\gamma_{\mathbf{G}}-x_2)\Bigg(-\frac{2}{\epsilon_1\Delta^3}+\frac{1}{\epsilon_1\epsilon_2\Delta^2}+\frac{1}{\epsilon_1^2\Delta^2}+\frac{1}{2\epsilon_2^2\epsilon_1\Delta}-\frac{1}{2\epsilon_1^2\epsilon_2\Delta}\Bigg)+\Phi^{(1)}_{3412}(1-x_1x_2x_3x_4\gamma_{\mathbf{G}})\Bigg(\frac{1}{2\epsilon_1^2\epsilon_2\Delta}\Bigg)\Bigg\} \tag{119}$$

and from the diagrams of Fig. 15 we have

$$T_{6aB}=\frac{J_\perp^4\sigma\sigma'}{J^3SN^2}\sum_{1,2,3,4,\mathbf{G}} l_1^2l_2^2l_3^2l_4^2\delta_{\mathbf{G}}c_1s_1c_2s_2\Bigg\{\Phi^{(7)}_{2413}(x_1x_3-\gamma_{\mathbf{G}}x_2x_4)\Bigg(-\frac{24}{\Delta^4}+\frac{8}{\epsilon_2\Delta^3}+\frac{4}{\epsilon_1\Delta^3}+\frac{2}{\epsilon_2^2\Delta^2}-\frac{2}{\epsilon_1\epsilon_2\Delta^2}-\frac{1}{\epsilon_2^2\epsilon_1\Delta}\Bigg)$$
$$+\Phi^{(3)}_{2413}(x_1x_2x_4\gamma_{\mathbf{G}}-x_3)\Bigg(-\frac{4}{\epsilon_1\Delta^3}+\frac{2}{\epsilon_1\epsilon_2\Delta^2}+\frac{1}{\epsilon_1\epsilon_2^2\Delta}\Bigg)$$
$$+\Phi^{(6)}_{1342}(x_3\gamma_{\mathbf{G}}-x_1x_2x_4)\Bigg(\frac{2}{\epsilon_1^2\Delta^2}-\frac{1}{\epsilon_1^2\epsilon_2\Delta}\Bigg)+\Phi^{(4)}_{4213}(x_2x_3-\gamma_{\mathbf{G}}x_1x_4)\Bigg(\frac{1}{\epsilon_2^2\epsilon_1\Delta}\Bigg)\Bigg\}, \tag{120}$$

where, in the term invoving $\Phi^{(6)}$ we interchanged momentum labels.

Finally, we consider the various contributions to T_{6b} from the diagrams of Fig. 16. The sums over energy denominators are similar to those of Fig. 9. So we get

$$T_{6b}=\frac{4J_\perp^4\sigma\sigma'}{J^3S}\frac{1}{N^2}\sum_{1,2,3,4}\delta_{\mathbf{G}}l_1^2l_2^2l_3^2l_4^2c_1^2s_1^2\Bigg[(\gamma_{\mathbf{G}}x_3x_4-x_1x_2)\Phi^{(7)}_{3412}\Bigg(\frac{1}{\Delta^3}-\frac{1}{\epsilon_1\Delta^3}-\frac{1}{4\epsilon_1^2\Delta^2}\Bigg)+(x_2-\gamma_{\mathbf{G}}x_1x_3x_4)\Phi^{(3)}_{3412}\Bigg(\frac{1}{\epsilon_1^2\Delta^2}\Bigg)\Bigg]. \tag{121}$$

We now use the relation in Appendix B to combine our results in the following compact way (For details see Appendix J Ref. 34):

$$\frac{E_{\mathrm{TOT}}}{2NJzS^2}=\frac{j^4\sigma\sigma'}{8S^3}\frac{1}{N^3}\sum_{1,2,3,4}\delta_{\mathbf{G}}l_1^2l_2^2l_3^2l_4^2\sum_{i=1,11}P(i)$$
$$\equiv\frac{j^4\sigma\sigma'}{8S^3}\sum_{i=1,11}E_i, \tag{122}$$

where $j\equiv(J_\perp/J)^4$ and $P(1)$ and $P(2)$ come from T_2:

$$P(1)=2\Bigg(\frac{4}{\Delta^3}-\frac{1}{\Delta^2\epsilon_1}-\frac{1}{\Delta^2\epsilon_2}+\frac{1}{\Delta\epsilon_1\epsilon_2}\Bigg)(x_1x_4-\gamma_{\mathbf{G}}x_2x_3)^2c_1s_1c_2s_2, \tag{123}$$

$$P(2)=-2\Bigg(\frac{1}{\Delta\epsilon_1\epsilon_2}-\frac{1}{\Delta^2\epsilon_1}-\frac{1}{\Delta^2\epsilon_2}\Bigg)\times(x_4-x_1x_2x_3\gamma_{\mathbf{G}})^2c_1s_1c_2s_2. \tag{124}$$

$P(3)$ and $P(4)$ come from combining T_3, T_4, T_{5a}, and T_{6b}:

$$P(3)=(\Phi^{(7)}_{3412})^2\Bigg(-\frac{8}{\Delta^5}+\frac{6}{\Delta^4\epsilon_1}+\frac{1}{\Delta^3\epsilon_1^2}\Bigg)c_1^2s_1^2, \tag{125}$$

$$P(4)=(\Phi^{(3)}_{3412})^2\Bigg(\frac{1}{\Delta^3\epsilon_1^2}\Bigg)c_1^2s_1^2. \tag{126}$$

$P(5)$, $P(6)$, $P(7)$, and $P(8)$ come from combining T_{6aA} and T_{5bA}:

$$P(5)=(\Phi^{(7)}_{3412})^2\Bigg(-\frac{12}{\Delta^5}+\frac{3}{\epsilon_1\Delta^4}+\frac{3}{\epsilon_2\Delta^4}+\frac{1}{2\epsilon_1^2\Delta^3}+\frac{1}{2\epsilon_2^2\Delta^3}-\frac{1}{\epsilon_1\epsilon_2\Delta^3}-\frac{1}{4\epsilon_1\epsilon_2^2\Delta^2}-\frac{1}{4\epsilon_1^2\epsilon_2\Delta^2}-\frac{1}{8\epsilon_1^2\epsilon_2^2\Delta}\Bigg)c_1s_1c_2s_2, \tag{127}$$

$$P(6)=(\Phi^{(3)}_{3412})^2\Bigg(\frac{1}{\epsilon_1^2\Delta^3}-\frac{1}{4\epsilon_1^2\epsilon_2^2\Delta}-\frac{1}{2\epsilon_1^2\epsilon_2\Delta^2}\Bigg)c_1s_1c_2s_2, \tag{128}$$

$$P(7)=-(\Phi^{(1)}_{3412})^2\Bigg(\frac{1}{8\epsilon_1^2\epsilon_2^2\Delta}\Bigg)c_1s_1c_2s_2, \tag{129}$$

$$P(8)=\Bigg(\frac{1}{8\epsilon_1^2\epsilon_2^2}\Bigg)[\Phi^{(7)}_{3412}(x_1x_2-\gamma_{\mathbf{G}}x_3x_4)+2\Phi^{(3)}_{3412}(x_1x_3x_4\gamma_{\mathbf{G}}-x_2)+\Phi^{(1)}_{3412}(1-x_1x_2x_3x_4\gamma_{\mathbf{G}})]c_1s_1c_2s_2. \tag{130}$$

$P(9)$, $P(10)$, and $P(11)$ come from combining T_{6aB} and T_{5bB}:

$$P(9)=\left\{(\Phi^{(7)}_{2413})^2\left(-\frac{24}{\Delta^5}+\frac{8}{\epsilon_2\Delta^4}+\frac{4}{\epsilon_1\Delta^4}+\frac{2}{\epsilon_2^2\Delta^3}-\frac{2}{\epsilon_1\epsilon_2\Delta^3}-\frac{1}{\epsilon_1\epsilon_2^2\Delta^2}-\frac{1}{4\epsilon_1^2\epsilon_2^2\Delta}\right)\right.$$
$$\left.+\frac{(x_1x_3-\gamma_{\mathbf{G}}x_2x_4)}{4\epsilon_1^2\epsilon_2^2}\Phi^{(7)}_{2413}\right\}c_1s_1c_2s_2, \tag{131}$$

$$P(10)=\left\{(\Phi^{(3)}_{2413})^2\left(\frac{2}{\epsilon_1^2\Delta^3}-\frac{1}{\epsilon_1^2\epsilon_2\Delta^2}-\frac{1}{2\epsilon_1^2\epsilon_2^2\Delta}\right)-\Phi^{(3)}_{2413}\frac{(x_3-x_1x_2x_4\gamma_{\mathbf{G}})}{2\epsilon_1^2\epsilon_2^2}\right.$$
$$\left.+\left(\frac{2}{\epsilon_1^2\Delta^2}-\frac{1}{\epsilon_1^2\epsilon_2\Delta}\right)(\Phi^{(3)}_{2413}+\gamma_{\mathbf{G}}\Phi^{(6)}_{1342})(x_3-x_1x_2x_4\gamma_{\mathbf{G}})\right\}c_1s_1c_2s_2, \tag{132}$$

$$P(11)=\left\{-\frac{1}{4\epsilon_1^2\epsilon_2^2\Delta}(\Phi^{(4)}_{2431})^2-\frac{1}{4\epsilon_1^2\epsilon_2^2}(x_1x_4-x_2x_3\gamma_{\mathbf{G}})\Phi^{(4)}_{2431}+\frac{(\epsilon_1-\epsilon_2)}{2\epsilon_1^2\epsilon_2^2\Delta}\Phi^{(4)}_{2431}(x_2x_3\gamma_{\mathbf{G}}-x_1x_4)\right\}c_1s_1c_2s_2. \tag{133}$$

It is not easy to check the correctness of this algebra. However, the fact that quite different mechanisms can be combined to yields results as in $P(3)$ or $P(4)$, for example, suggests that these terms, at least, are correct. Such a resulting form (in terms of squares of the non-Hermitian matrix element) was found previously in a complicated spin-wave calculation.[37]

To determine the numerical values of these sums we divided each of the nine momentum integrals into a sum over a mesh of n points. Our work up to $n=28$ showed that these values could be extrapolated to $n=\infty$ by each sum to a form $A+B/n$. We thereby found

$$\{10^7E_i\}=\{169,-603,5627,233,\ -2987,99,$$
$$-1210,0,52,2668,-45\} \tag{134}$$

and $\Sigma_iE_i=4.00\times10^{-4}$ gives the energy in Eq. (122). The uncertainty in these results is at the level of a percent or so. [The result that the term in $P(8)$ vanishes is obtained analytically in Appendix M of Ref. 34.] The fact that this sum is positive, indicates that second-neighboring layers have lower energy when they are out of phase. One may well ask whether or not there is some simple argument which could indicate the sign of the result. Had we obtained a nonzero result at order S, we could have reproduced the answer qualitatively by a calculation in which we neglected the propagation of modes: we could have treated spin waves as Einstein (localized) excitations.[29,30] To obtain a result at order 1 we would have to take account of spin-wave interactions (whereby the energy of two localized modes would be different when the excitations are on neighboring sites as contrasted to being separated). To obtain a result at order $1/S$ from a localized calculation would require a very involved calculation, from which one would not learn more than from the present calculation.

V. DISCUSSION

In deriving our results, it may seem that our results rely on the assumption that the ground state is a collinear structure by analogy with the previous results of Shender[4] and of Rastelli *et al.*[27,28] However, to avoid relying on such an assumption, we performed a more general calculation at order j^2 in which we assigned an arbitrary orientation (specified by a unit vector $\hat{n}_p$) for the staggered magnetization in the pth plane. A calculation following the methods of Sec. III yielded the result

$$\Delta e=-\langle r^2+p^2\rangle_{\mathbf{q}}j^2\sum_{p=1}^{M-1}[1+(\hat{n}_p\cdot\hat{n}_{p+1})^2], \tag{135}$$

as expected. At order j^2 we recover the expected result that the fluctuation energy at order j^2 selects collinear states. Thus we were justified to treat a collinear model to discuss the way the remaining degeneracy within collinear structures was resolved.

In many cases of interest, e.g., in the cuprate antiferromagnets, the assumption that one has dominantly antiferromagnetic planes which are weakly coupled by interplane interactions has the result that $j=J_\perp/J$ is small enough that j^6/S is very much less than j^4/S^3. In that case, the calculation of Sec. IV becomes relevant. As it happens, both the contributions of order j^6/S and those of order j^4/S^3 indicate a lower energy when alternate planes are antiferromagnetically coupled. Thus we think that this result does hold for a range of parameters in the Heisenberg model with only nearest-neighbor interactions. If one includes a direct coupling, J_3, between second-neighboring planes, the energy of this interaction $[\Delta e\sim(J_3/J)]$ must be compared to that found here due to indirect interactions. Since such interactions come from overlap of wave functions, it is possible that J_3/J is comparable to j^4. Needless to say, in real systems

many other small energies, such as dipolar energies would also have to be considered.[26]

We may summarize our conclusions as follows:

(1) We have calculated the contributions to the energy which distinguish between various orderings of antiferromagnetic planes in the bct antiferromagnet with weak nearest-neighbor interplane interactions $J_\perp$. At second order in $j=J_\perp/J$, where J is the in-plane interaction, the energy favors collinear structures, as expected from previous calculations.

(2) If we write the quantum zero-point energy, E_Q as $E_Q=E_C[1+\Delta e_Q]$, where E_C is the classical ground-state energy of a single plane, then Δe_Q can be calculated as a perturbation series in j and $1/S$. At first order in $1/S$, the leading contribution to Δe_Q which involves the configuration of the planes (assumed to be collinear) is of order j^6, as written in the abstract. For systems consisting of more than four layers, this energy favors second-neighboring planes being antiparallel. Thus the entire structure has only the degeneracy associated with the relative phase of the odd-numbered layers relative to the even numbered layers. This degeneracy reflects a true symmetry of the system and cannot be removed.

(3) At order j^4, the leading contribution to Δe_Q which involves the configurations of the layers is of order $1/S^3$ and is given by the complex expressions of Sec. IV. Numerical evaluation of this result shows that this energy also favors second-neighboring layers being antiparallel.

(4) An interesting result is found for a system consisting of a small number of bct layers. In particular, for a three-layer system, we find that the first and third layers are parallel to one another in the ground state. It would also be interesting to study experimentally a system with four bct layers. In that case our results indicate that all configurations in which both next-nearest neighboring planes are parallel are degenerate with those in which both next-nearest neighboring plnaes are antiparallel. Although this degeneracy will no doubt be removed by higher-order effects, it does suggest the possibility of obtaining unusual spin structures in extremely thin-film systems.

(5) We mention a caution that in real systems there may be other energies,[26] such a single ion anisotropy, dipolar, or further-neighbor interactions, which might be more important than those discussed here. In particular, for La_2CuO_4, experiments[38] show that the Dzyaloshinskii-Moriya anisotropy determines the three dimensional spin structure.

(6) In Ref. 4 it was shown that the most important effect of quantum fluctuations was to introduce an effective biquadratic exchange interaction between sublattices of the form written in Eq. (1). In agreement with Ref. 4 for the bcc case, this effective interaction can be shown[20] to give rise to nonzero frequencies of the ''optical'' modes at zero wave vector in which sublattices do not precess in phase. Because the collinearity energy (which is of order $J_\perp^2/J$) is much larger than the energy which determines how spins in alternate planes orient relative to each other, these optical mode frequencies are essentially determined by the collinearity energy of Eq. (1) and are not very sensitive to the global spin structure.

ACKNOWLEDGMENTS

Work at the University of Pennsylvania was supported in part by the National Science Foundation under Grant No. DMR-91-22784. A.B.H. would like to thank Theoretical Physics, Oxford University and the Physics Department of Tel Aviv University for their hospitality. He also acknowledges support from EPSRC (UK) and a grant from the USIEF. The authors wish to thank E. Rastelli for pointing out some mistakes in the paper as originally submitted.

APPENDIX A: NONLINEAR MATRIX ELEMENTS

We first discuss the phase factor in Eq. (25). For illustrative purpose we consider only the first term in $H_p^{(4)}$ (which we denote T_1) and for simplicity we temporarily omit the indices p. Then

$$\begin{aligned} T_1 &= -\frac{2J}{N^2}\sum_{1,2,3,4;\delta_1,i\in \text{ up}} a^+(1)a(-2)b^+(3)b(-4) \\ &\quad\times e^{i[\mathbf{r}_i\cdot(1+2+3+4)+(3+4)\cdot\delta_1]} \\ &= -\frac{2J}{N}\sum_{1,2,3,4;\mathbf{G}} \delta_{\mathbf{G}} a^+(1)a(-2)b^+(3)b(-4) \\ &\quad\times e^{i\tau_1(\mathbf{p})\cdot\mathbf{G}}\gamma_{3+4}, \end{aligned} \tag{A1}$$

where $i\in$ up means that $\mathbf{r}_i$ is summed only over the positions of up spins [as in Eq. (5)] and we noted that all positions were referred to $\tau_1(p)$. Alternatively, we could refer positions to $\tau_2(p)$ in which case we would have

$$\begin{aligned} T_1 &= -\frac{2J}{N^2}\sum_{1,2,3,4;\delta_1,i\in \text{ down}} a^+(1)a(-2)b^+(3)b(-4) \\ &\quad\times e^{i[\mathbf{r}_i\cdot(1+2+3+4)+(1+2)\cdot\delta_1]} \\ &= -\frac{2J}{N}\sum_{1,2,3,4;\mathbf{G}} \delta_{\mathbf{G}} a^+(1)a(-2)b^+(3)b(-4) \\ &\quad\times e^{i\tau_2(\mathbf{p})\cdot\mathbf{G}}\gamma_{1+2}. \end{aligned} \tag{A2}$$

These are equivalent because when $1+2+3+4+\mathbf{G}=0$, then

$$e^{i\tau_1(p)\cdot\mathbf{G}}\gamma_{3+4}=e^{i\tau_2(\mathbf{p})\cdot\mathbf{G}}\gamma_{1+2}. \tag{A3}$$

Similarly, we discuss Eq. (28). We have

$$V_{\mathrm{NL}}(p+1,p) = -J_{\perp}\sum_{p,i,j} b(p;i)a^{+}(p+1;j)a(p+1;j)a(p+1;j)\,\gamma^{(U)}_{p,p+1}(i,j)$$

$$= -5\frac{J_{\perp}}{N^2}\sum_{p,j,i\in\text{down}}\sum_{1,2,3,4} b_p(-1)a^{+}_{p+1}(2)a_{p+1}(-3)a_{p+1}(-4)\,\gamma^{(U)}_{p,p+1}(i,j)e^{i\mathbf{q}_1\cdot\mathbf{r}_i}e^{i(\mathbf{q}_2+\mathbf{q}_3+\mathbf{q}_4)\cdot\mathbf{r}_j}$$

$$= -\frac{J_{\perp}}{N^2}\sum_{p,j,i\in\text{down}}\sum_{1,2,3,4} b_p(-1)a^{+}_{p+1}(2)a_{p+1}(-3)a_{p+1}(-4)\,\gamma^{(U)}_{p,p+1}(i,j)$$

$$\times e^{i(\mathbf{q}_1+\mathbf{q}_2+\mathbf{q}_3+\mathbf{q}_4)\cdot\mathbf{r}_i}e^{-i(\mathbf{q}_2+\mathbf{q}_3+\mathbf{q}_4)\cdot(\mathbf{r}_i-\mathbf{r}_j)}$$

$$= -\frac{2J_{\perp}}{N}\sum_{1,2,3,4,\mathbf{G}}\delta_{\mathbf{G}}e^{i\mathbf{G}\cdot\tau_2(p)}\gamma^{(U)}_{p,p+1}(\mathbf{q}_2+\mathbf{q}_3+\mathbf{q}_4). \tag{A4}$$

APPENDIX B: RELATIONS FOR Φ

Here we give some relations between the DM coefficients which we used to obtain the forms given in the summary:

$$\Phi^{(8)}_{1234}+\Delta(x_1x_2-\gamma_{\mathbf{G}}x_3x_4)=\Phi^{(7)}_{3412}, \tag{B1}$$

$$\Phi^{(2)}_{1234}-(\Delta-2\epsilon_1)(x_2-\gamma_{\mathbf{G}}x_1x_3x_4)=\Phi^{(3)}_{3412}, \tag{B2}$$

$$\Phi^{(1)}_{1234}+(\Delta-2\epsilon_1-2\epsilon_2)(1-x_1x_2x_3x_4\gamma_{\mathbf{G}})=\Phi^{(1)}_{3412}, \tag{B3}$$

$$\Phi^{(3)}_{2413}-\gamma_{\mathbf{G}}\Phi^{(6)}_{1342}=(x_3-\gamma_{\mathbf{G}}x_1x_2x_4)(2\epsilon_1-\Delta), \tag{B4}$$

and

$$\Phi^{(4)}_{2431}-\Phi^{(4)}_{3124}=(x_1x_4-\gamma_{\mathbf{G}}x_2x_3)(\epsilon_1+\epsilon_2-\epsilon_3-\epsilon_4). \tag{B5}$$

A derivation of these relations is given in Appendix L of Ref. 34.

[1] E. F. Shender and P. C. W. Holdsworth, in *Fluctuations and Order: The New Synthesis*, edited by M. Milonas (Springer-Verlag, Berlin, 1995).

[2] J. Villain, R. Bidaux, J. P. Carton, and R. Conte, J. Phys. (Paris) **41**, 1263 (1980).

[3] C. L. Henley, J. Appl. Phys. **61**, 3962 (1987).

[4] E. Shender, Sov. Phys. JETP **56**, 178 (1982).

[5] A. B. Harris and E. Rastelli, J. Phys. C **20**, L741 (1987).

[6] C. L. Henley, Phys. Rev. Lett. **62**, 2056 (1989).

[7] N. D. MacKenzie and A. P. Young, J. Phys. C **14**, 3927 (1981).

[8] J. L. Lebowitz, M. K. Phani, and D. F. Styer, J. Stat. Phys. **38**, 413 (1985).

[9] A. Gukasov, T. Brueckel, B. Dorner, V. Plakhty, W. Prandl, E. F. Shender, and O. P. Smirnov, Europhys. Lett. **7**, 83 (1988).

[10] A. P. Ramirez, Annu. Rev. Mater. Sci. **24**, 453 (1994).

[11] K. Kubo and T. Kishi, J. Phys. Soc. Jpn. **60**, 567 (1991).

[12] C. Broholm, G. Aeppli, G. P. Espinosa, and A. S. Cooper, Phys. Rev. Lett. **65**, 3173 (1990).

[13] A. B. Harris, C. Kallin, and A. J. Berlinsky, Phys. Rev. B **45**, 2899 (1992).

[14] E. F. Shender, V. B. Cherepanov, P. C. W. Holdsworth, and A. J. Berlinsky, Phys. Rev. Lett. **70**, 3812 (1993).

[15] D. A. Huse and A. D. Rutenberg, Phys. Rev. B **45**, 7536 (1992).

[16] S. Sachdev, Phys. Rev. B **45**, 12 377 (1992).

[17] J. N. Reimers, J. E. Greedan, R. E. Kremer, E. Gmelin, and M. A. Subramanian, Phys. Rev. B **43**, 3387 (1991).

[18] A. B. Harris, C. Micheletti, and J. M. Yeomans, Phys. Rev. Lett. **74**, 3045 (1995).

[19] Y. Yamamoto and T. Nagamiya, J. Phys. Soc. Jpn. **32**, 1248 (1972).

[20] T. Yildirim, A. B. Harris, and E. F. Shender (unpublished).

[21] R.J. Birgeneau and G. Shirane, *Physical Properties of High Temperature Superconductors*, edited by D. M. Ginsberg (World Scientific, Singapore, 1989).

[22] T. Thio, T. R. Thurston, N. W. Preyer, P. J. Picone, M. A. Kastner, H. P. Henssen, D. R. Gabbe, C. Y. Chen, R. J. Birgeneau, and A. Aharony, Phys. Rev. B **38**, 905 (1988).

[23] For a review, see J. W. Lynn, in *Physical and Material Properties of High Temperature Superconductors*, edited by S. K. Malik and S. S. Shah (Nova Science, New York, 1994), p. 243.

[24] Y. Tokura, H. Takagi, and S. Uchida, Nature (London) **337**, 345 (1989).

[25] D. Vaknin, S. K. Sinha, C. Stassis, L. L. Miller, and D. C. Johnston, Phys. Rev. B **41**, 1926 (1990).

[26] T. Yildirim, A. B. Harris, A. Aharony, and O. Entin-Wohlman, Phys. Rev. Lett. **72**, 3710 (1994).

[27] E. Rastelli, S. Sedazzari, and A. Tassi, J. Phys. Condens. Matter **1**, 4735 (1989).

[28] E. Rastelli, S. Sedazzari, and A. Tassi, J. Phys. Condens. Matter **2**, 8935 (1990).

[29] A. B. Harris, in *Disorder in Condensed Matter Physics*, edited by J. A. Blackman and J. Taguena (Clarendon, Oxford, 1991).

[30] M. W. Long, J. Phys. Condens. Matter **1**, 2857 (1989).

[31] A. B. Harris, D. Kumar, B. I. Halperin, and P. C. Hohenberg, Phys. Rev. B **3**, 961 (1971).

[32] F. J. Dyson, Phys. Rev. **102**, 1217 (1956); S. V. Maleev, Sov. Phys. JETP **6**, 776 (1958).

[33] A perfectly consistent labeling of spins specifying both their position and also whether they are up or down is awkward. Our notation is that we label all spins with a scalar index i which assumes odd values, say, for up spins and even values for down spins. Thus one should interpret $a(p;i)$ to be zero if i is even and $b(p;i)=0$ if i is odd.

[34] See AIP document no. PAPS PRBMDO-53-6455-48 for 48 pages of caluclation of $J_\perp^4$ terms. Order by PAPS number and journal reference from American Institute of Physics, Physics, Auxiliary Publication Service, Carolyn Gehlbach, 500 Sunnyside Boulevard, Woodbury, New York, 11797. Fax: 516-576-2223, e-mail: janis aip.org. The price is $1.50 for each microfiche (98 pages) or $5.00 for phtocopies of up to 30 pages, and $0.15 for each additional page over 30 pages. Airmail additional. Make checks payable to the American Institute of Physics.

[35] G. Baym and A. M. Sessler, Phys. Rev. **131**, 2345 (1963). R. Balian and C. DeDominicis, C. R. Acad. Sci. **250**, 3285 (1960); A. A. Abrikosov, L. P. Gorkov, and I. Y. Dzyaloshinskii, *Quantum Field Theoretical Methods in Statistical Physics*, 2nd ed. (Pergamon, New York, 1965).

[36] We use two conventions for labeling lines in diagrammatic perturbation theory. In the first convention, we give only the layer number associated with the line. When we feel that more concrete information is needed we label the line according to the type of excitation (α or β) as well as the giving the layer index. In such cases we find it convenient to label lines within the convention that α, β, γ, δ, ρ, and η denote, respectively, α_1, β_1, α_2, β_2, α_3, and β_3.

[37] A. B. Harris, Phys. Rev. **183**, 486 (1969).

[38] T. Thio *et al.*, Phys. Rev. B **38**, 905 (1988).